JOC The Journal of Organic Chemistry

Article

C#(*S*/*R*)-Bimodal Peptide Nucleic Acids (C#-*bm*-PNA) form Coupled Double Duplexes by Synchronous Binding to Two complementary DNA Strands

Pramod Bhingardeve, Krishna N. Ganesh, and Bharath Raj Madhanagopal

J. Org. Chem., **Just Accepted Manuscript** • DOI: 10.1021/acs.joc.0c01853 • Publication Date (Web): 28 Sep 2020

is published by the American Chemical Society. 1155 Sixteenth Street N.W., Washington, DC 20036

Cγ(*S*/*R*)-Bimodal Peptide Nucleic Acids (Cγ-*bm*-PNA) form Coupled Double Duplexes by Synchronous Binding to Two complementary DNA Strands

Pramod Bhingardeve,[a] Bharath Raj Madhanagopal,[b] and Krishna N Ganesh[a,b,*]

a. Indian Institute of Science Education and Research (IISER) Pune, Dr Homi Bhabha Road, Pune 411008, India
b. Indian Institute of Science Education and Research (IISER) Tirupati, Karkambadi Road, Mangalam, Tirupati, 517507, India.

* To whom correspondence should be addressed. kn.ganesh@iisertirupati.ac.in

ABSTRACT

Peptide nucleic acids (PNA) are linear equivalents of DNA with a neutral acyclic polyamide backbone that has nucleobases attached via t-amide link on repeating units of aminoethylglycine. They bind complementary DNA or RNA with sequence specificity to form hybrids that are more stable than the corresponding DNA/RNA self duplexes. A new type of PNA termed bimodal PNA [Cγ(4*S*/*R*)- *bm*-PNA] is designed to have a second nucleobase attached via amide spacer to a sidechain at Cγ on the repeating *aeg* units of PNA oligomer. Cγ-Bimodal PNA oligomers that have two nucleobases per *aeg* unit is demonstrated to concurrently bind two different complementary DNAs, to form duplexes from both t-amide side and Cγ-side. In such PNA:DNA ternary complexes, the two duplexes share a common PNA backbone. The ternary DNA **1**:Cγ(*S*/*R*)-*bm*-PNA:DNA **2** complexes exhibit better thermal stability than the isolated duplexes, and the Cγ(*S*)-*bm*-PNA duplexes are more stable than Cγ(*R*)-*bm*-PNAs duplexes. Bimodal PNAs are first examples of PNA analogues that can form DNA2:PNA:DNA1 double duplexes via recognition through natural bases. The conjoined duplexes of Cγ-bimodal PNAs can be used to generate novel higher level assemblies.

INTRODUCTION

Peptide nucleic acids (PNA) are synthetic DNA analogues with an acyclic polyamide backbone. PNA strands recognize the nucleobase sequences of complementary DNA and RNA to yield highly stable derived PNA:DNA and PNA:RNA duplexes.[1,2] The non-chiral PNA backbone consists of recurring units of aminoethyl glycine (*aeg*) and in each *aeg* unit, one of the nucleobases (A/T/C/G) is attached via tertiary amide function (Figure 1a). In PNA, the distance between the neighbouring nucleobases is similar to that in DNA/RNA. This feature

alongwith absence of charges, allows the PNA strands to form sequence-specific base pairing with the complementary DNA/RNA strands.[3] The resulting PNA duplexes with complementary DNA/RNA have superior stability and sequence fidelity compared to that of normal DNA duplexes.[4] These attributes of PNA and its unique property of strand invasion[5] of DNA duplexes have been exploited in various applications including diagnostics[6] and antisense therapeutics.[7] The simplicity of the PNA backbone provides ample opportunities for its structural variations and modulation of functional selectivity via conjugation with ligands for cell recognition and transport across membrane. [8,9] The structural modifications involve functionalization at Cα and Cγ on the *aeg* backbone as they do not adversely impact the complementation of PNA with DNA/RNA.[8-10] In particular, PNAs that carry cationic alkylamino, guanidino and polyethylene glycol substitutions at Cα or Cγ show better DNA-binding and cell-penetration.[10,11] Another class of modifications involve constraining the *aeg* unit through cyclization giving rise to substituted 5-membered proline/pyrrolidine rings or fused cyclopentyl or cyclohexyl moieties on backbone, which may conformationally pre-organize the backbone for preferential hybridization with DNA or RNA.[8b,12]

In this work, we have now embarked on a new strategy to enhance the versatility of standard *aeg*-PNAs through installation of a second nucleobase on a sidechain hosted at Cγ of each *aeg* unit in PNA backbone (Figure 1b). Such PNA analogues (termed bimodal *bm*-PNA) bear two nucleobases per *aeg* unit of PNA and can ideally form two duplexes (Figure 1c), one from t-amide linked bases (as in normal PNA) and another from Cγ-sidechain linked nucleobases, both duplexes sharing the common *aeg* backbone. Further, the distance between neighbouring nucleobases anchored on successive Cγ-Cγ sites (Figure 1c) is similar to that between adjacent bases on t-amide chains of standard PNA. This geometrical compatibility facilitates the concurrent binding of two DNA sequences one from each side. Employing such an analogy with Cα sites on PNA backbone, we have recently demonstrated that Cα-*bm*-PNA (Figure 1e) possessing nucleobases attached to sidechain at Cα through a triazole linker can indeed form double duplexes (Figure 1f) providing the proof of concept.[13] In this manuscript, we show that Cγ(*S*/*R*)-*bm*-PNAs with nucleobases anchored on Cγ-sidechain in both *S*/*R* configuration also recognize DNA from both sides, endorsing the generality of bimodal PNA concept. Unlike many other DNA analogues, the simplicity of PNA backbone is ideally suited to host two nucleobases per repeating unit. A previous approach to host two nucleobases on DNA backbone via linkage at C4/C5 of sugar residue or at C5 of pyrimidine base (double headed DNA) showed destabilization of derived DNA:DNA single duplexes and no attempt

was made to hybridize the anchored base sequence with another complementary DNA to form second duplex.[14] The bimodal PNAs described here are conceptually quite different from DNA / PNAs made with synthetic Janus bases[15] that recognize two strands of DNA from two faces of nucleobase, which have recently found interesting applications.[16] In our designs of bimodal PNAs, natural bases are anchored on both t-amide and on Cγ-sidechain (and at Cα-sidechain[13]) with the backbone acquiring a Janus character for recognizing different complementary DNAs from two sides. The control *iso*-PNAs (Figure 1d) wherein the nucleobases reside only on Cγ–sidechain (and on Cα-sidechain[13]), devoid of bases on t-amide link are new isomorphic PNA analogues that can independently form duplexes with DNA.

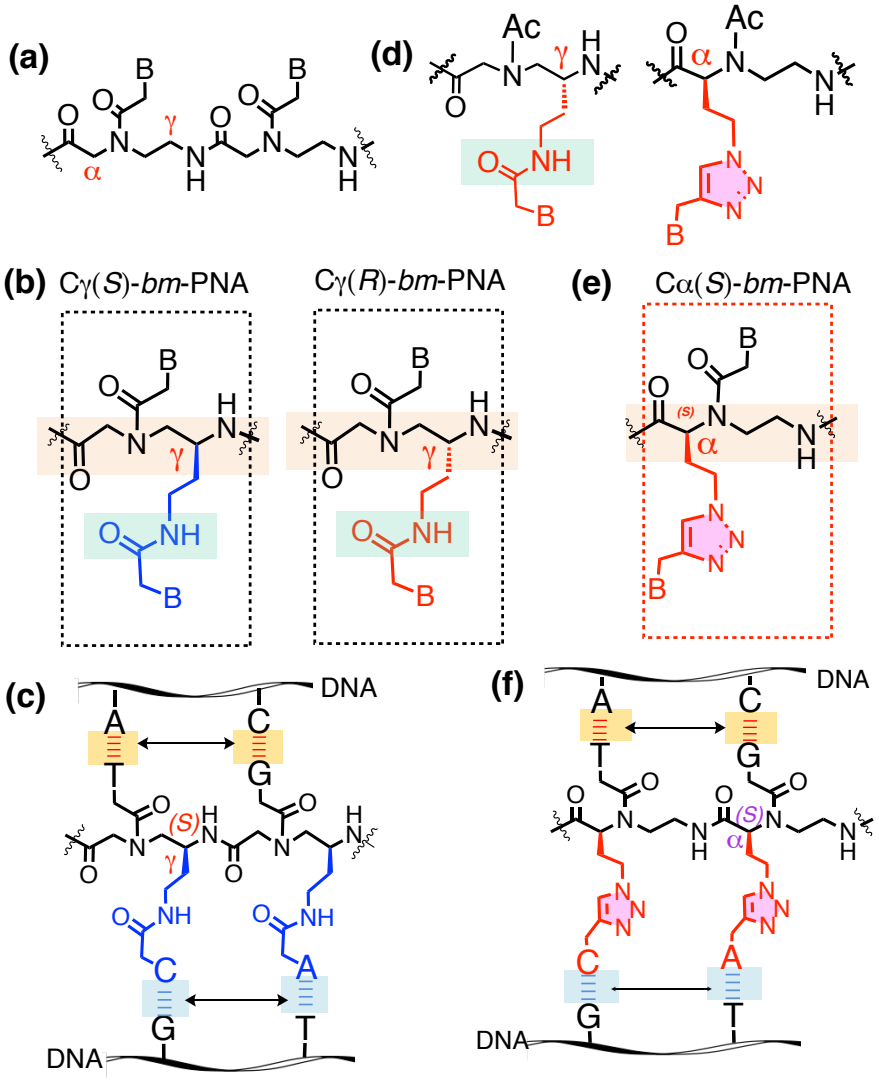

Figure 1. (a) *aeg*-PNA (b) Cγ(*S*/*R*)-*bm*-PNA (c) Cγ-*bm*-PNA:DNA double duplex (d) Cγ and Cα-*iso*-PNA (e) Cα(*S*)-*bm*-PNA and (f) Cα-*bm*-PNA:DNA double duplex, B = T/A/G/C

The target Cγ(*S*/*R*)-*bm*-PNAs **1** and **2** (Figure 2) have 8 nucleobases (GT_6C) linked via t-amide sidechain as in standard PNA and each *aeg* unit carries a second nucleobase on sidechain at Cγ of ethylenediamine component. The nucleobase bearing ethylamido sidechain at Cγ in both *S* [Cγ(*S*)-*bm*-PNA **1**] and *R* [Cγ(*R*)-*bm*-PNA **2**] stereochemistry were synthesised for comparison, although it is known that Cγ(*S*) substituents are better for hybridization with DNA.[8e,11a] The choice of spacer at Cγ and the base sequences was due to ease of synthesis and provide proof of the new concept rather than any structural or functional considerations. Unsubstituted *aeg*-PNA-C/G unit was included at N and C- termini to avoid steric interference during synthesis or in hybridization. The control Cγ(*S*/*R*)-*iso*-PNAs (**3** and **4**) are new isomeric PNA structures that bear nucleobases only on Cγ-sidechain with absence of t-amide linked nucleobases. They were used to test their independent abilities to base pair with DNA.

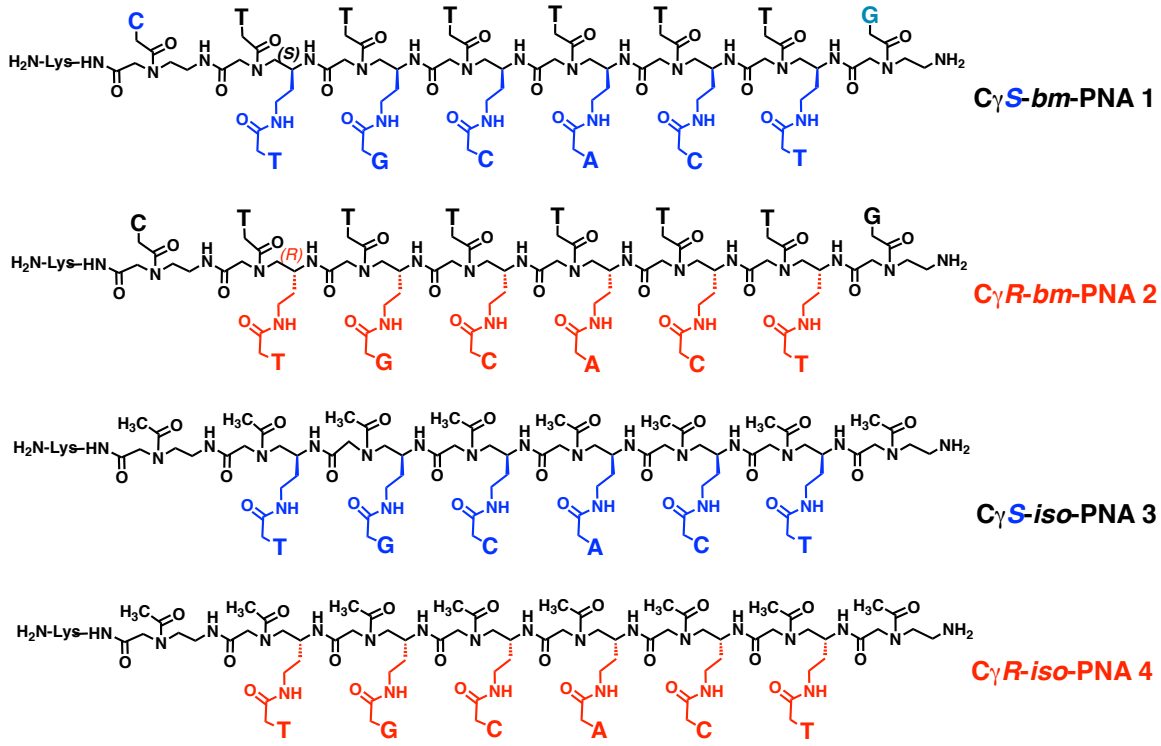

Figure 2. Structures of Cγ(*S*/*R*)-*bm*-PNAs and Cγ(*S*/*R*)-*iso*-PNAs

RESULTS AND DISCUSSION

Synthesis of monomers Cγ(*S*/*R*)-*bm* and Cγ(*S*/*R*)-*iso* PNA monomers 1-4

The Cγ(*S/R*)-*bm* PNA monomers **1** and **2** that carry t-amide linked nucleobases on *aeg* backbone with orthogonal amino protecting groups (NH-Boc on backbone and Fmoc on Cγ-ethylamino sidechain) and Cγ(*S/R*)-*iso* PNA monomers **3** and **4** that have nucleobases only at Cγ sidechain (Figure 3) were used for solid phase synthesis of target bimodal PNAs (Figure 2). The amino groups on nucleobases were suitably protected (iBu for 2-NH_2 of G, Cbz for 6-NH_2 of A and 4-NH_2 of C), and can all be deprotected in a single step on the resin**.**

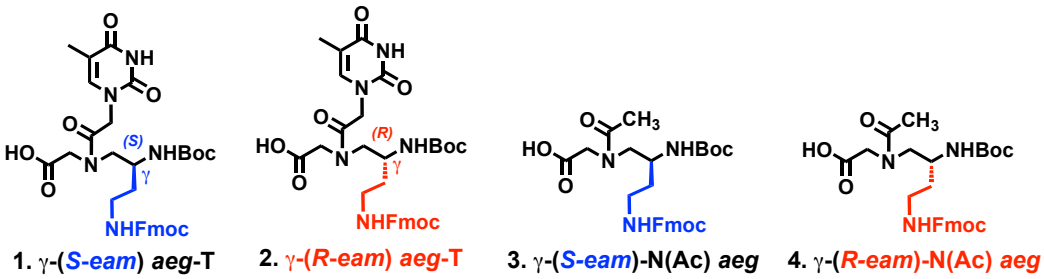

Figure 3. Structures of protected monomers employed for the synthesis of *iso*-PNA and bimodal PNA oligomers on solid phase. *eam* – ethylamino; *aeg* – aminoethylglycyl

The bimodal PNA monomers **1** and **2** with Cγ(*S/R*) sidechain were synthesized starting from L-glutamine and D-Glutamine as per synthetic route shown in Scheme 1. The Cγ(*S*)-*bm*-PNA monomer **1** was synthesised from compound **5** which was prepared from commercial L-glutamine. The reaction of ester **5** with aq, LiOH in MeOH gave the acid **6**.[17] The NHCbz protecting group in **6** was exchanged to NHFmoc to maintain orthogonality required for solid phase synthesis. This was achieved by first hydrogenating **6** in presence of Pd/C in methanol to give the free amine, which was in situ reprotected using Fmoc-Cl and 10% aq. Na_2CO_3 in THF to yield the desired *S*-*bm*-PNA monomer **1.**

The synthesis of Cγ(*R*)-*bm*-PNA monomer **2** was done starting from D-glutamine **7** which was first protected at α-NH_2 by reaction with Boc_2O to yield α-*NH*-Boc-D-glutamine **8** (Scheme 1). This was followed by the reaction of 2(*R*)-NHBoc-D-glutamine **8** with iodobenzene diacetate (PIDA) which led to the formation of 2(*R*)-NHBoc-4-aminobutanoic acid **9**. Reaction of compound **9** with CBzCl in toluene containing $NaHCO_3$ produced the orthogonally protected 2(*R*)-NHBoc-4-(NHCbz)-aminobutanoic acid **10** in quantitative yield. It was converted using dimethyl sulfate to methyl ester **11**, which was reduced using sodium borohydride in absolute ethanol to give the alcohol **12**. The primary hydroxyl group in **12** was reacted with mesyl chloride in DCM in the presence of triethyl amine to obtain the O-mesylate

derivative **13**, which was immediately reacted with sodium azide in dry DMF to convert it to the azide **14**. The reduction of azide function using Raney Ni under hydrogenation conditions yielded the free amine that was reacted with α-bromoethylacetate in-situ to obtain the alkylated compound **15**. The N-chloroacetylation of secondary amine in **15** was achieved by its reaction with chloroacetyl chloride to get **16** that was condensed with thymine to afford the Cγ(*R*)-(NHFmoc-aminoethyl)-(NHBoc-aminoethyl) ethyl glycinate **17** in good yield. The appearance of peaks at δ 7.05 ppm and 1.87 ppm in ^{1}H NMR confirmed the presence of thymine in product **17.** Subsequently, the ester was hydrolysed using 10% aq. LiOH/MeOH to obtain the acid **18**, which was hydrogenated in presence of Pd/C to yield the free amine. This was in-situ protected using Fmoc-Cl and 10% aq. Na_2CO_3 in THF to generate the desired Fmoc derivative **2.**

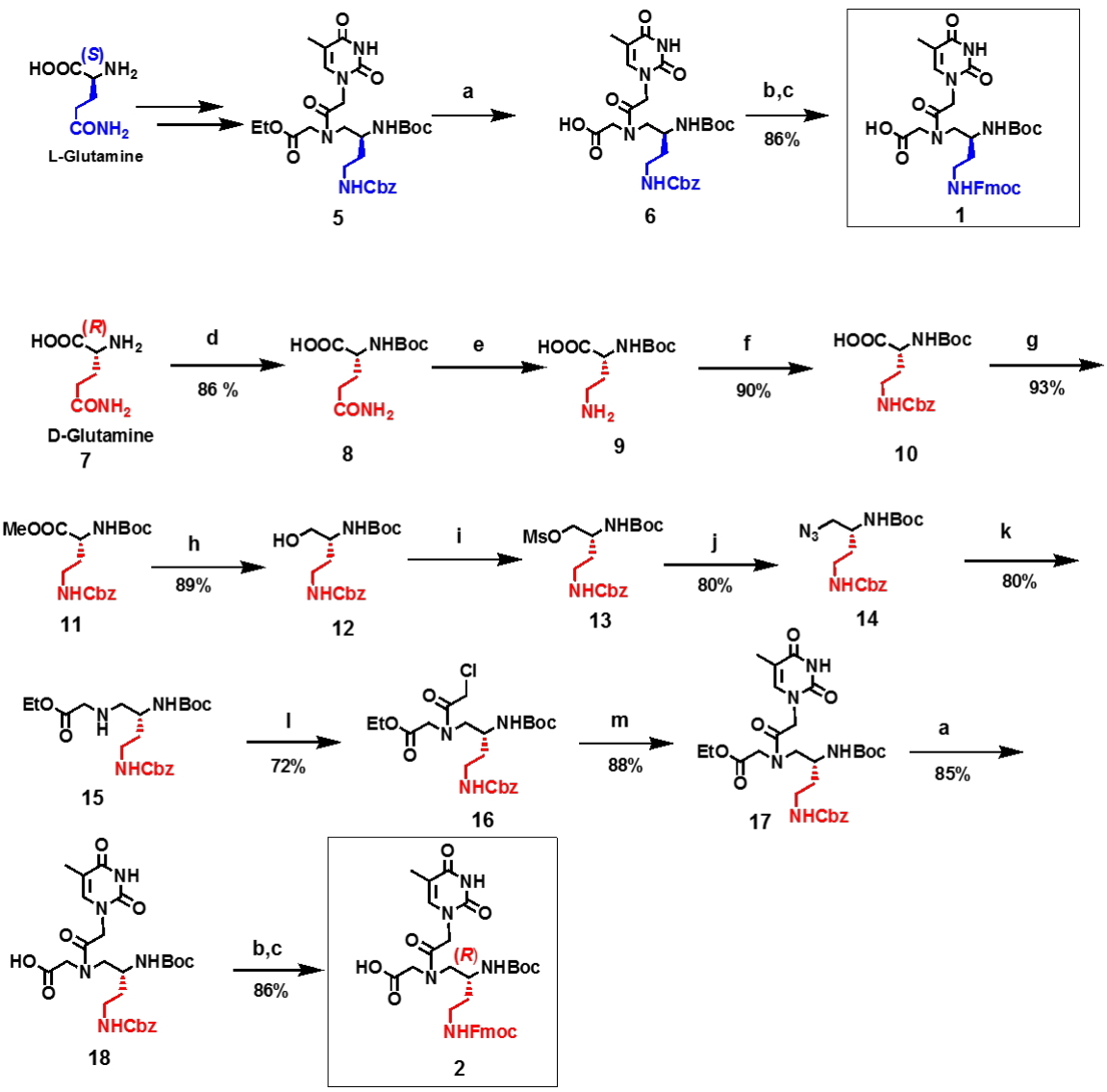

Scheme 1. a.. 10% aq. LiOH, MeOH,3 h. **b**. Pd-C/H_2, MeOH, 4 h; **c**. Fmoc-Cl, Na_2CO_3, THF-H_2O; 4 h; **d.** $(Boc)_2O$, NaOH, Dioxane, 1 h; **e**. $PhI(OAc)_2$, EA:ACN:H_2O (2:2:1); **f**. Cbz-Cl, $NaHCO_3$, Acetone; **g**. Me_2SO_4, K_2CO_3, Acetone, 4 h, 55 °C; **h**. $NaBH_4$, EtOH, 4 h; **i**. MsCl, TEA, DCM, 0 °C; **j**. NaN_3, DMF, 80 °C, 8 h; **k**.H_2, RaNi/EtOH, 80 h; Ethylbromoacetate, ACN, TFA, 12 h; **l.** Chloroacetyl chloride, TEA, DCM, 8 h; **m**. Thymine, K_2CO_3, DMF, 8h.

The monomer **3** necessary for synthesis of Cγ(*S*)-*iso*-PNA **3** oligomer (Figure 2) was prepared by route as shown in Scheme 2. Compound **19** an intermediate in the synthesis of **6**[17] was N-acetylated to obtain **20** followed by hydrolysis of ester to yield the acid **21**. The N-Cbz function in **21** was deprotected by hydrogenation to the corresponding free amine which was in-situ deprotected with the base labile Fmoc group to obtain the orthogonally protected monomer **3**. The Cγ(*R*)-*iso*-PNA monomer **4** was synthesized by a similar set of reactions starting from compound **15** as shown Scheme 2. NMR (^{1}H and ^{13}C) and mass spectral data (ESI, S13-S31) were used to characterize the structures of all intermediates and monomers.

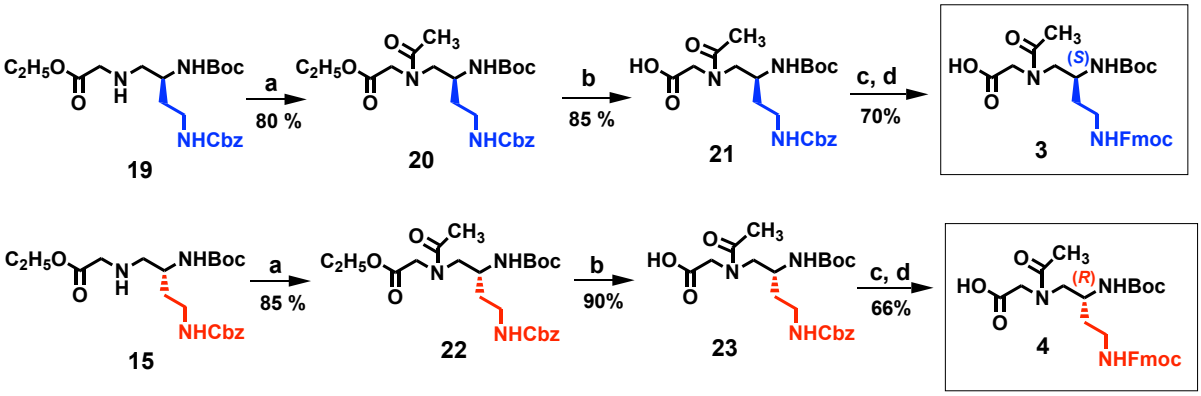

Scheme 2. Synthesis of Cγ(*S*/*R*)-*iso*-PNA monomers **3** and **4** needed for assembly of Cγ(*S*)-*iso*-PNA **3** oligomer and Cγ(*R*)-*iso*-PNA **4** oligomers**;** **a**. DhbtOH, AcOH, DCM, 12 h; **b**. 10% aq. LiOH, MeOH,3 h.; **c** H_2, Pd-C; **d** Fmoc-Cl, aq. $NaHCO_3$, 2 h.

Solid phase synthesis of Cγ(*S*/*R*)-bimodal and *iso*-PNA oligomers

The bimodal PNAs Cγ(*S*)-*bm*-PNA **1** and Cγ(*R*)-*bm*-PNA **2** having identical base sequences but with different stereochemistry at Cγ (Figure 2) were assembled on MBHA resin using solid phase synthesis protocols,[18] employing a combination of Boc (backbone) and Fmoc (sidechain) strategy (Scheme 3). The PNAs were synthesized starting from C-terminus using orthogonally protected monomers, Cγ(*R*)-*bm* monomer **2** for Cγ(*R*)-*bm*-PNA **2** oligomer and Cγ(*S*)-*bm* monomer **1** for Cγ(*S*)-*bm*-PNA **1** oligomer. The sequence of steps employed for the solid phase synthesis of Cγ(*S*/*R*)-*bm*-PNAs is illustrated in Scheme 3. The synthesis was initiated with first coupling on MBHA resin with the orthogonally protected L-lysine

(ω NHCBz,α NHBoc) as the C-terminal spacer amino acid. This was followed by deprotection of α NHBoc to yield free NH_2 group on resin, which was coupled with *aeg*-PNA-C monomer and deprotected with TFA to regenerate free NH_2 function on the resin. From this stage, each backbone coupling was done by either Cγ(*S*)-ethylamino-PNA monomer **1** for Cγ(*S*)-*bm*-PNA **1** or Cγ(*R*)-*bm*-PNA monomer **2** for Cγ(*R*)-*bm*-PNA **2**. The coupling of appropriate monomer was followed by deprotection of Fmoc to free NH_2 group on Cγ-sidechain for subsequent coupling with desired ($A^{Cbz}/C^{Cbz}/G^{iBu}$/T)-acetic acid (shown in color) as per the sequence. Successive cycles of couplings with monomer (**1** or **2**) and Fmoc deprotection (step **a**) and nucleobase-acetic acid coupling and Boc deprotection (step **b**) were continued in stepwise manner to build the target Cγ(*S*/*R*)-*bm*-PNA oligomers. The final coupling was done with unmodified PNA-G monomer. All coupling reactions were done under microwave conditions to enhance the efficiency of coupling reactions. The protocol in Scheme 3 was also used for synthesis of Cγ(*S*)-*iso*-PNA **3** from monomer **3** and Cγ(*R*)-*iso*-PNA **4** from monomer **4**. Finally, TFA-TFMSA (step **c**) was used to cleave the synthesized Cγ(*S*/*R*)-*bm*-PNA and *iso*-PNA oligomers from the resin. The PNA oligomers were purified using RP-HPLC and characterized by mass spectral data Table 1 and ESI (S5-S9). The sequence of steps employed for solid phase synthesis of Cγ(*S*)-*bm*-PNA **1** oligomer is shown in Supporting Information (ESI, Scheme 2).

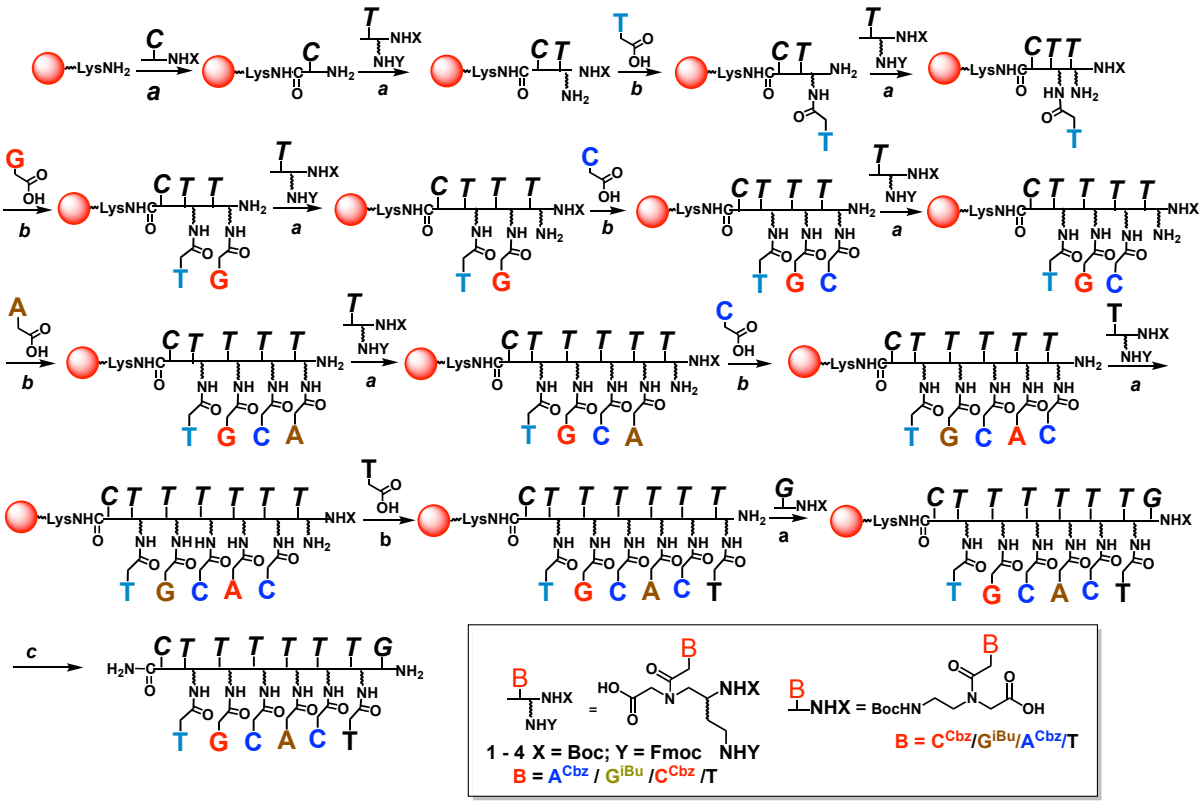

Scheme 3. Common protocol for synthesis of Cγ(*S*/*R*)-*bm*-PNA oligomers from monomers **1** and **2** and Cγ(*S*/*R*)-*iso*-PNA oligomers from monomers **3** and **4**. Wavy line represents Cγ sidechain with *S* or *R* stereochemistry. Typical coupling reaction: Microwave 25 W, 5 min, rt 6 h. The resin 10 mg (~0.2 mmol/g), monomers (12 mg, 3 eq) **a** (i) HOBt (6 mg, 3 eq), HBTt (6 mg, 3 eq), DIPEA (10 µL), DMF (ii) 20% piperidine in DMF; **b** (i) HOBt, HBtU, DIPEA, DMF (ii) 50% TFA in DCM; **c** TFA-TFMSA. Coupling of monomers on t-amide side shown by bold italics (in black) and coupling on Cγ-side shown by bold letters (in colour) for bases A,T, C and G.

Table 1. MALDI-TOF spectral data of Cγ-*iso*- and Cγ-*bm*-PNA oligomers

Entry	PNA Oligomers	Mol. formulae	HPLC Rt	Calcd. Mass	Obs. Mass
1	Cγ-*S*-*bm*-PNA **1**	$C_{145}H_{187}N_{65}O_{44}$	13.3	3543.43$[M + H]^+$	3542.50
2	Cγ-*R*-*bm*-PNA **2**	$C_{145}H_{187}N_{65}O_{44}$	13.5	3543.43 $[M + H]^+$	3543.07
3	Cγ-*S*-*iso*-PNA **3**	$C_{112}H_{136}N_{70}O_{19}$	13.1	2580.79 $[M + K]^+$	2580.69
4	Cγ-*R*-*iso*-PNA **4**	$C_{112}H_{136}N_{70}O_{19}$	13.5	2580.79 $[M + K]^+$	2580.66

Thermal stability of Cγ(*S*/*R*)-*bm* and *iso*(*S*/*R*)-PNA:DNA duplexes

The Cγ(*S*/*R*)-*bm*-PNA and Cγ(S/*R*)-*iso*-PNA oligomers were independently hybridised with DNA **1** or DNA **2** that are complementary to Cγ-side and t-amide side base sequences respectively to generate different Cγ-amide duplexes with DNA **1** (Figure 4, **A**-**B**, **D**-**E**) and t-amide duplexes with DNA **2** (Figure 4, **C**-**F**). When both DNA **1** and DNA **2** are present, the bimodal Cγ(*S*/*R*)-*bm*-PNAs can form double duplexes (Figure 4, **G** and **H**). After mixing the PNA and DNA components in appropriate stoichiometry, the samples were annealed by heating the mixtures to 80 °C in buffer at pH 7.2 and cooled slowly to room temperature to enable efficient hybridization. The DNA sequences (DNA **1** and DNA **2**) were chosen to yield PNA:DNA antiparallel duplexes in which the N-terminus of PNA is oriented towards the 3' end of DNA. The thermal stabilities of various duplexes were obtained by recording UV absorbance at 260 nm by continuous variation of temperature. The melting temperatures (T_ms) of the PNA:DNA hybrids were extracted from the corresponding UV-T plots (Figure 5).

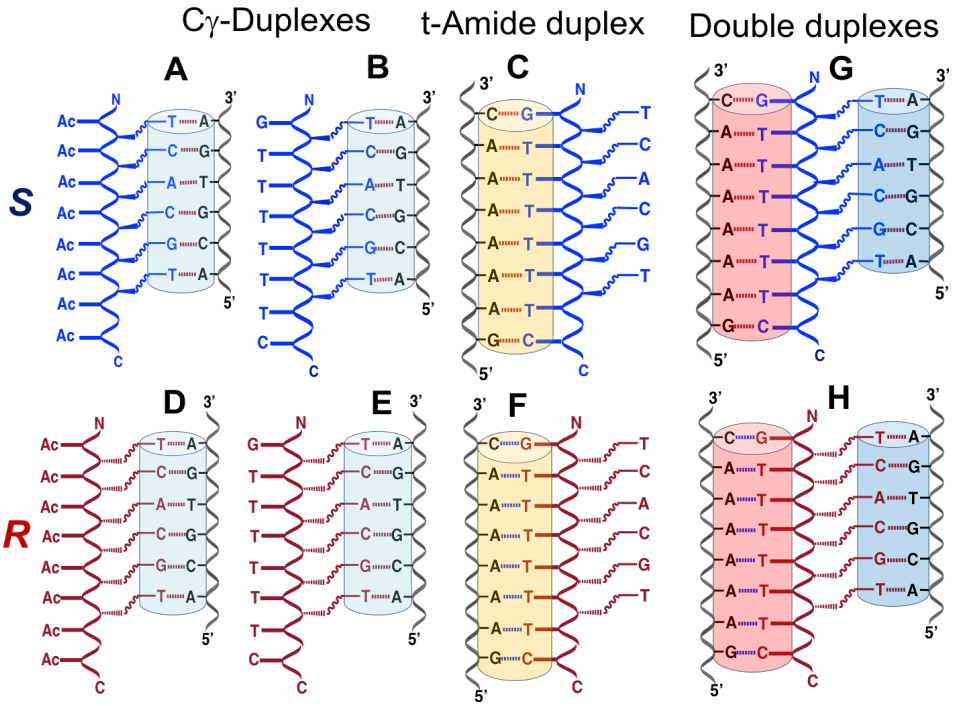

Figure 4. *iso*-PNA and *bm*-PNA duplexes**. A**. Cγ(*S*)-*iso*-PNA **3**:DNA **1**; **B.** Cγ(*S*)-*bm*-PNA **1**:DNA **1**; **C**. DNA **2**:Cγ(*S*)-*bm*-PNA **1**; **D**. Cγ(*R*)-*iso*-PNA **3**:DNA **1; E.** Cγ(*R*)-*bm*-PNA **2**:DNA **1; F.** DNA **2**:Cγ(*R*)-*bm*-PNA **2; G.** DNA **2**:Cγ(*S*)-*bm*-PNA **1**:DNA **1** (double duplex); **H**. DNA **2**:Cγ(*R*)-*bm*-PNA **2**:DNA **1** (double duplex)

***iso*-PNA and *bm*-PNA single duplexes with DNA.** The establishment of PNA:DNA duplexes is confirmed by the observed sigmoidal transitions in UV-T plots,[18,19] in which the melting point T_m of duplexes correspond to the midpoint of transitions. This was determined from the the first derivative plot in which the maximum provides a more accurate estimation of the T_m value (Figure 5). The single sigmoidal transitions seen for Cγ-*iso*-PNA duplexes **A** and **D** clearly indicate that the new isomeric PNA structure carrying nucleobases only on Cγ can form perfect duplex with DNA **1**. The (*S*)-*iso*-PNA **3** duplex (**A**) has higher stability (T_m 49.2 °C) than the (*R*)-*iso*-PNA **4** duplex (**D**, T_m 42.2 °C) with ΔT_m (*S*-*R*) of +7 °C. The designed (*S*/*R*) bimodal PNAs also formed corresponding Cγ-amide Cγ(*S*)-*bm*:PNA:DNA **1** (**B**) and Cγ(*R*)-*bm*:PNA:DNA **1** (**E**) duplexes with T_ms of 51.7 °C and 38.1 °C respectively. These data suggest that the presence of unpaired nucleobases on t-amide side can influnece the stability of Cγ-amide duplexes. The Cγ(*S*)-*bm*:DNA **1** duplex (**B**) had a higher melting (+2.5 °C) than the corresponding (*S*)-*iso*-PNA:DNA **1** duplex (**A**), while Cγ(*R*)-*bm*:DNA **1** duplex (**E**) had a lower melting (-4.1 °C) than (*R*)-*iso*-PNA:DNA **1** duplex (**D**). The Cγ(*S*/*R*)-*bm*-PNAs also formed duplex on t-amide side with DNA **2** similar to that of standard PNA:DNA duplexes, with T_ms

of 45.5 °C for Cγ(*S*)-*bm* duplex (**C**) and 33.4 °C for Cγ(*R*)-*bm* duplex (**F**) respectively; again the *S*-duplex was significantly more stable than *R*-duplex by +12.1 °C. Thus stereocenter at Cγ dictates the stability of individual duplexes derived from *iso*-PNAs and Cγ-*bm*-PNAs. The results are consistent with the literature reports that Cγ(*S*) substitution stabilises PNA:DNA duplexes better than Cγ(*R*)-substitution.[11] Significantly, the present results demonstrate that bases attached on sidechain at Cγ on backbone instead of t-amide link on *aeg* backbone (as in standard PNA) can successfully form duplexes, both in the new isomeric *iso*-PNA and in the designed Cγ-bimodal PNA.

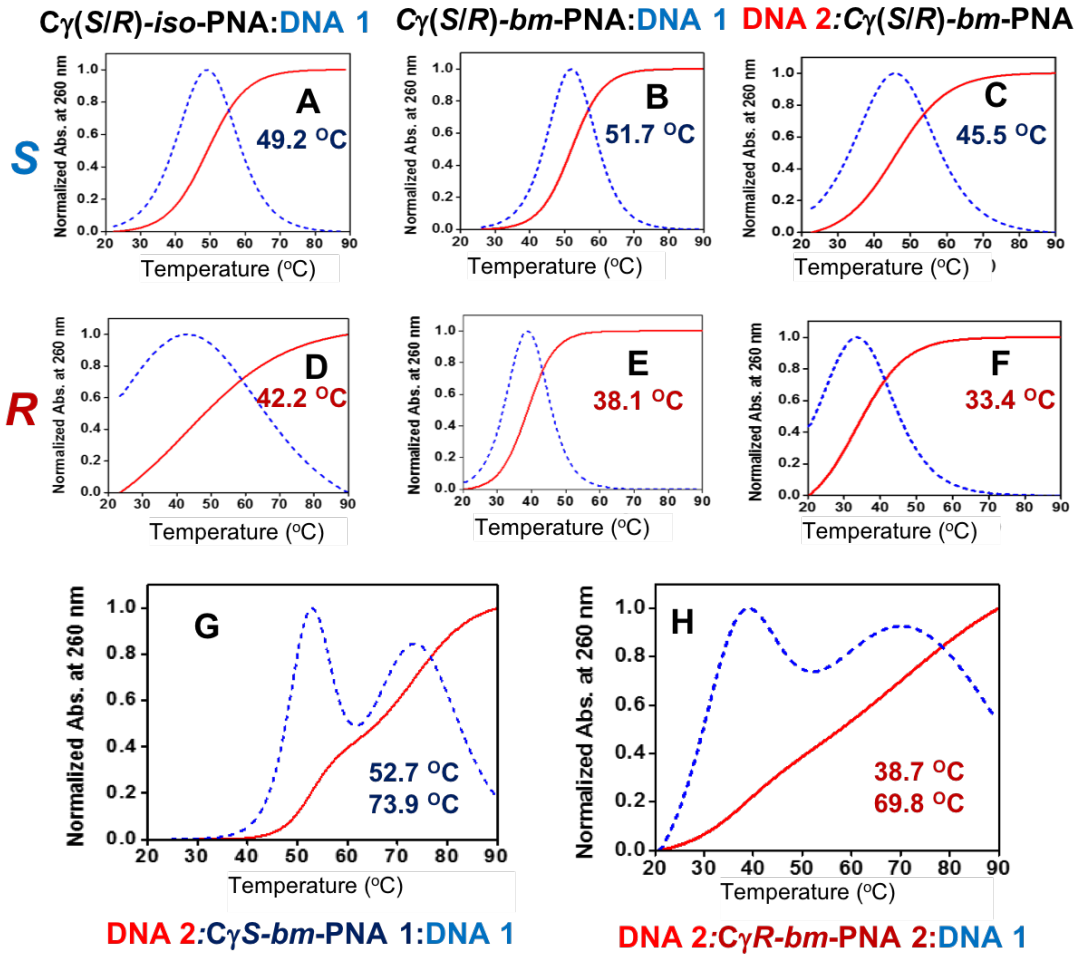

Figure 5. UV-melting and first derivative plots of duplexes. Normalised melting curve (red line) and first derivative plots (blue dashed line). Numbers in plots correspond to T_m of duplexes.

Double duplex from Cγ(S/R)-bm-PNA:DNA complexes. The Cγ(*S*/*R*)-*bm*-PNAs were hybridized with an equimolar mixture of DNA **1** complementary to Cγ-side and DNA **2**

complementary to t-amide side. Figure 5 (**G** and **H)** shows the melting curves of the derived hybrids. In contrast to single sigmoidal melting noticed for single duplexes, both complexes exhibited double sigmoidal melting, indicating the presence of two distinct transitions. The T_ms of 52.7 ºC and 73.9 ºC (Figure 5**G**) for the ternary complex DNA **2**:Cγ(*S*)-*bm*-PNA:DNA **1** are higher than the T_ms of the corresponding isolated duplexes. Similarly, the ternary complex PNA:DNA DNA **2**:Cγ(*R*)-*bm*-PNA:DNA **1** (Figure 5**H**) from *R*-bimodal PNA exhibited two T_ms at 38.7 ºC and 69.8 ºC. Though the transitions are broad, they are well resolved, with distinct and discernible transitions having difference in T_ms of 21.2 ºC for *S*-*bm*-PNA complex and 31.1 ºC for *R*-*bm*-PNA complex. The ternary complex in both Cγ(*S*) and Cγ(*R*) *bm*-PNAs are more stable than the individual binary complexes by >20 ºC. The double sigmoidal UV-T_m pattern indicated the melting process to be biphasic (three state) and can originate from either a sequential melting of two duplexes as in DNA triplexes[19] or simultaneous disassociation of both DNA strands from PNA as in PNA_2:DNA melting.[20] A sequential melting process for two duplexes should not have any influence on the second transition since after the dissociation of first DNA strand from the ternary complex, the melting of second duplex should be similar to that of the corresponding isolated duplex. A single step dissociation of ternary complex as in PNA_2:DNA triplexes[20] should lead to only a single transition representing true melting of ternary complex. Since both T_ms in each bimodal (*S*/*R*) PNA:DNA_2 complex (**G**/**H**) are higher than individual duplexes (**B**,**C**/**D**,**E**) the melting process of two duplexes are coupled to each other, mutually enhancing their stability. The difference in the T_ms of higher transitions of the ternary complexes of Cγ(*S*)-*bm*-PNA **1** and Cγ(*R*)-*bm*-PNA **2** is +4 °C, which is 3-times less than the difference in T_ms of their isolated duplexes [ΔT_m(**B**–**E**) Cγ-amide: +13.6 °C; (**C**–**F)** t-amide: +12.1°C). Thus the formation of ternary complexes compensates the larger difference in thermal stabilitites of individual Cγ(*R*) and Cγ(*S*) duplexes.

Mismatch C(γ)-bm-PNA:DNA duplexes. The sequence fidelity in the complementation of base-pairing from Cγ-side in *bm*-PNA:DNA duplexes was examined by determining the T_ms of mismatched duplexes. Cγ(*S*/*R*)-*bm*-PNAs (**1** and **2**) were hybridized individually with DNA **1m** (5'-AGCGCA-3') and DNA **2m** (5'-GAAAC AAC-3') that carry single C:A base mismatch on Cγ-side and t-amide side respectively (ESI, S11-S12). All mismatched duplexes showed lower T_ms compared to perfect duplexes. (Figure 6, green bars). The mismatch duplex Cγ(*S*)-*bm*-PNA **1**:DNA **1m** was destabilized by (−)13 ºC and Cγ(*R*)-*bm*-PNA **1**:DNA **1m** duplex destabiized by (−)3.9 ºC. The corresponding t-amide mismatch duplexes with DNA **2m** also

showed lower stability with ΔT_ms of (−)11.3 ºC and (−)3.6 ºC for *S*-*bm* PNA **1** for *R*-*bm*-PNA **2** respectively. In the corresponding mismatched double duplexes from Cγ(*S*)-*bm*-PNA **1** and Cγ(*R*)-*bm*-PNA **2**, the two transitions collapsed into single transitions with T_ms of 61.5 ºC and 52.3 ºC, with detsbilization ΔT_ms of (−)12.4 ºC and (-)17.5 ºC respectively (Figure 6). Thus, in mismatched bimodal complexes, both DNA strands clearly dissociate in single step, similar to that in PNA_2:DNA triplex.[20] Notably, even in the set of mismatched complexes, the T_m of ternary complex [DNA **2m**:Cγ(*S*/*R*)-*bm*-PNA:DNA **1m**] was higher than the T_ms of isolated duplexes, substantiating the generality of enhanced stability in double duplexes. Compared to perfect duplexes, the destabilization seen in mismatched duplexes of *S*-*bm*-PNA were almost similar to destabilization per base mismatch seen in unmodified PNA:DNA duplexes.[19] This substantiated that co-existence of two duplexes sharing a common PNA backnone as in bimodal PNA:DNA_2 ternary complexes mutually confer higher stabilty on each other.

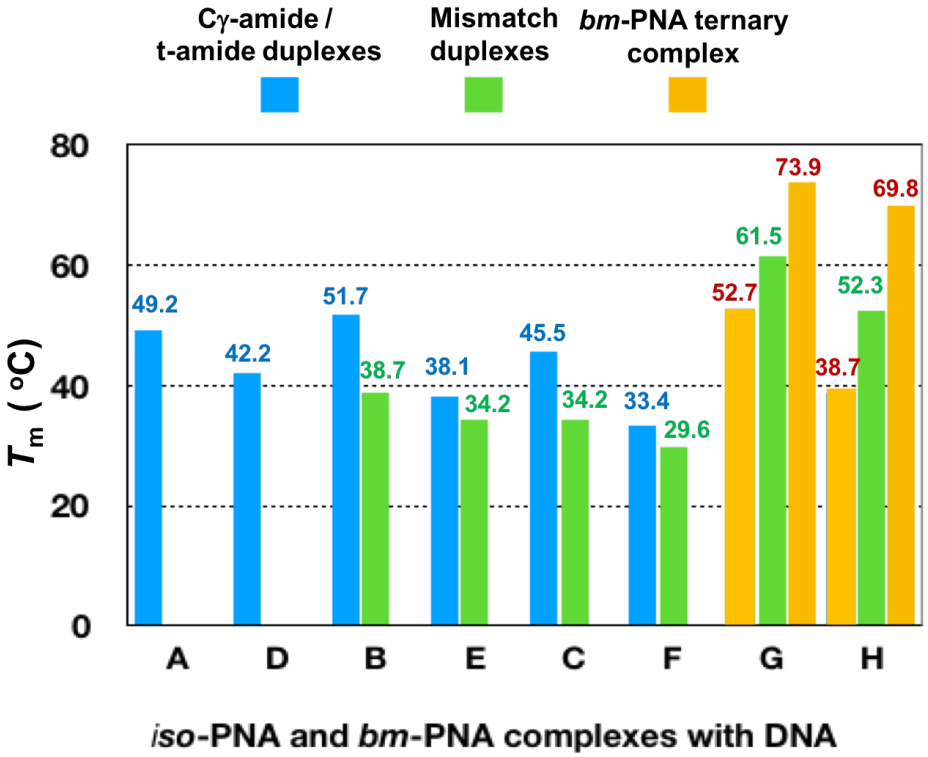

Figure 6. Comparative T_ms of duplexes and ternary complexes. Labels on X-axis correspond to duplexes shown in in Figure 5

CD spectra of Cγ-*bm*-PNA:DNA duplexes

The CD spectral profiles of Cγ(*S*/*R*)-*bm*-PNA duplexes and double duplexes (Figure 7) resemble the characteristic CD profiles of PNA:DNA duplexes,[21] with minor changes in relative intensities among the duplexes and double duplexes. The double duplexes (green curve) indicated prominent positive bands at 265 nm and 218-220 nm. The Cγ(*S*)-*bm*-PNA **1** exhibited relatively higher band at 260 nm, suggesting a better stacking of bases compared to that in Cγ(*R*)-*bm*-PNA **2**. The handedness of two stereomeric Cγ(*S*/*R*)-*bm*-PNA:DNA duplexes remain same as both of them have L-lysine at C-terminus and the CD spectra are dominated by DNA contribution with well-established right handedness of DNA:PNA duplexes. The chiral effects Cγ (*S*) and Cγ(*R*) on PNA backbone seems to be weak to influence the handedness of base stacks and the stability of derived duplexes are affected through minor conformational effects. The CD spectra also ruled out the formation of any *bm*-PNA$_2$:DNA **2** triplexes arising from t-amide side of bimodal PNAs.

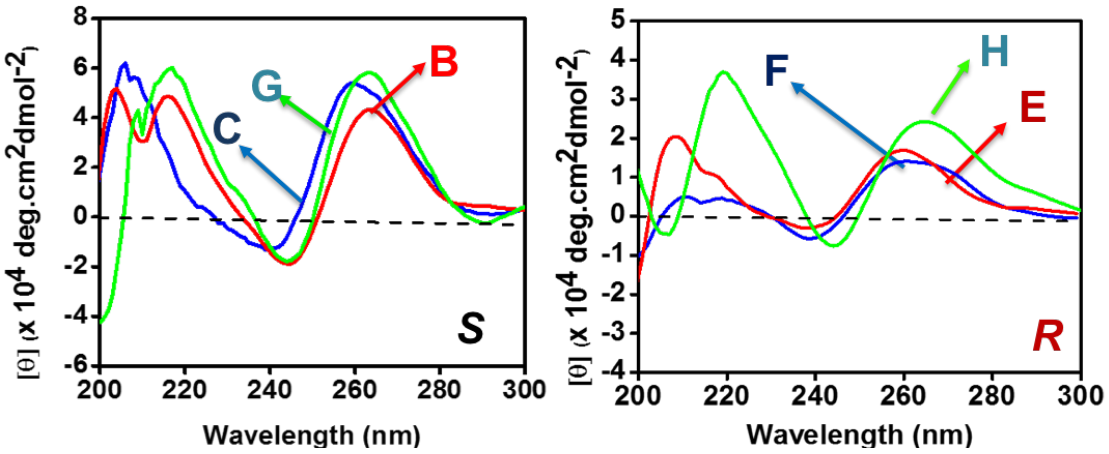

Figure 7. CD spectra of Cγ-*bm*-PNA:DNA duplexes. Labels for duplexes as in Figure 4.

Plausible dissociation model for bimodal PNA:DNA ternary complexes

The double sigmoidal transition seen in bimodal PNA:DNA$_2$ duplexes with both T_ms higher than that of isolated duplexes is interesting and results in enhanced stability of both duplex components of the ternary complex. As mentioned earlier, this observation does fit not into either a sequential melting model (like in DNA triplexes) or simulatneous dissociation model (as in PNA$_2$:DNA triplexes). It may be mentioned that in PNAs that carry Janus bases and bind two DNA strands, the original stability of individual duplexes was retained (Figure 4 in ref 16b). The origin of double melting process in bimodal PNAs, which do not retain the original duplex stability, may be ascribed to a process of premelting in the ternary complex

during the first transition, followed by complete melting during the second transition. Such premelting processes are well documented in DNA duplexes and involves co-operative perturbations in base stacking accompanied by non-cooperative changes in sugar-phosphate backbone conformation.[22] In the intermediate conformations adopted during premelting transitions termed *premeltons*[22d] the bases retain H-bonding with slight distortion. In DNA-drug interactions, this may involve additional reorganization in the spine of hydration. Premelting transitions are quite broad and ultimately lead to sharp transition with complete dissociation of both strands through breaking of H-bonds.

The kinetics of association – dissociation transition of PNA:DNA hybrids is slow and leads to broad melting transitions. In Cγ-*bm*-PNA:DNA_2 complex where two duplexes share a common PNA backbone, the premelting of the tight ternary complex would involve partial unwinding of both duplexes with co-operative unstacking of bases accompanied by changes in PNA backbone conformation. The unwinding of the complex with destacking of bases may lead to the first transition. (Figure 8, path A). Compared to DNA:DNA duplexes, the pre-melting transition in bimodal PNA:DNA_2 double duplexes, seems to be more prominent. This is due to a tighter winding of two duplexes that co-operatively uncoil with a greater degree of unstacking of bases. The two DNA strands are still held in place by H-bonding between nucleobases of bimodal PNA. The common PNA backbone thus couples the premelting of the two duplexes which is followed by complete dissociation in a subsequent step to result in second transition. The mismatched ternary complex yields only a single transition, with the mismatches on both sides presumably relieving the strain compared to the tight perfect double duplex. A similar pattern of double transitions with T_ms higher than the isolated duplexes were also seen with Cα-*bm*-PNA,[13] suggesting the generality of the phenomenon. The difference in the T_ms of the *S* and *R* ternary complexes [Cγ(*S*)-*bm*-PNA **1** and Cγ(*R*)-*bm*-PNA **2**] is only 4 °C, about 3 times lower than the T_m differences between the respective isolated duplexes [ΔT_m Cγ-amide (**B**-**E**): 13.6 °C and t-amide (**C**-**F**), 12.1 °C)]. This points to the additional stabilizing effects arising when the two duplexes are coupled through a shared backbone, which also overrides the lower stabilizing effects in Cγ(*R*) stereomeric duplex compared to Cγ(*S*) duplex. Understanding the structure and biophysical origin of two transitions in bimodal PNA ternary complexes and their higher stability compared to isolated duplexes needs further experimentation such as identifying the intermediates by careful temperature dependent CD experiments and computational studies.

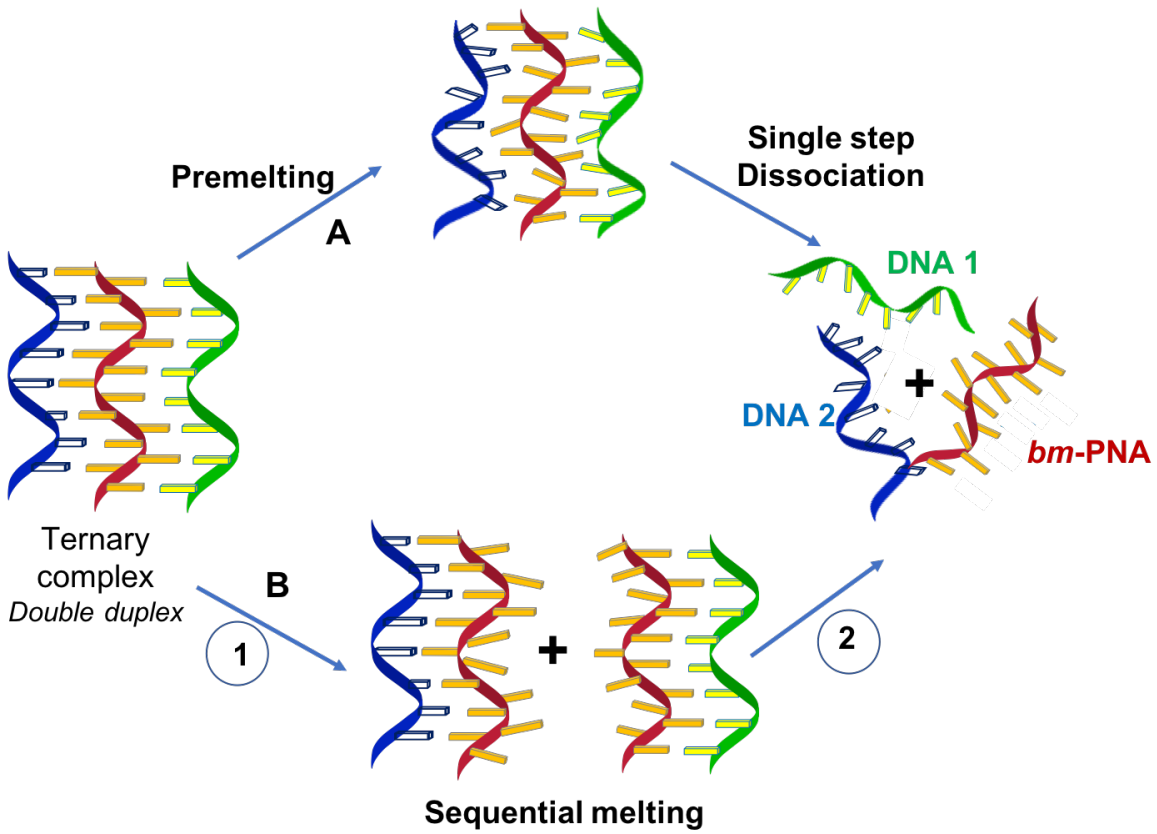

Figure 8. Cartoon representation of (A) pre-melting-dissociation and (B) sequential dissociation models for melting of bimodal PNAs

CONCLUSIONS

A new type of PNA derivatives termed "bimodal PNA"s intended to concurrently hybridise to two complementary DNA strands have been designed by installing a set of nucleobases on Cγ-sidechain of each *aeg* repeating unit of the standard PNA oligomer. The orthogonally protected (Fmoc/Boc) stereomeric Cγ(*S*/*R*)-bimodal PNA monomers were employed for solid phase synthesis of bimodal Cγ(*S*/*R*)-*bm*-PNA oligomers having mixed bases on both sides. Cγ-*iso*-PNA monomers with bases only on Cγ-sidechain on *aeg* backbone were used for synthesis of isomeric Cγ(*S*/*R*)-*iso*-PNA oligomers. The UV-melting data on (*S*/*R*)-*iso*-PNA:DNA hybrids suggested formation of stable duplexes from the new isomeric PNA that is devoid of nucleobases linked to the t-amide as in *aeg*-PNA.

The designed bimodal Cγ(*S*/*R*)-*bm*-PNAs individually bind DNAs complementary on each side to yield the corresponding binary Cγ-amide and t-amide duplexes. Together, they hybridize on both sides of bimodal PNA backbone to generate ternary complexes, which show

biphasic double transition with higher stability compared to independent duplexes. Cγ(*S*)-dupexes show significantly higher stability than Cγ(*R*) duplexes. The enhanced T_ms in two step melting of ternary complex suggests neither a sequential melting mechanism as in DNA triplexes or by a single step simultaneous dissociation as in PNA_2:DNA triplexes. The complete dissociation of ternary complex is perhaps preceded by a pre-melting transition involving a partial unstacking of bases and backbone conformational change (Figure 8). The UV-melting profiles of Cγ(*S*/*R*)-*bm*-PNA double duplexes observed in this work are consistent with that we recently reported for Cα-*bm*-PNA,[13] validating the generality of the design principles of bimodal PNAs to create two duplexes that are structurally coupled with a shared PNA backbone. The proposed mechanism of dissociation of such structurally coupled double duplexes needs further study.

The Cγ-*bm*-PNA duplexes studied here along with recently published Cα-*bm*-triazole PNA oligomer[13] are first examples of PNA derivatives in which single PNA backbone hosts two PNA:DNA duplexes through base pairing of natural bases. The base pairing of nucleobases on Cα and Cγ-sidechains are probably Watson−Crick type, because of the high duplex stability and sequence specificity. This was further substantiated by lower T_ms in mismatched duplex. The control *iso*-PNAs (Cγ and Cα-*iso*-PNAs[11]) are new isomorphs of PNAs that successfully form strong duplexes and open avenues for studying entirely new types of PNA:DNA complexes. Based on the choice of the sequences on either side (polypurines/polypyrimidines/G_n/C_n), the Cγ and Cα-bimodal PNAs can be used to generate welded PNA:PNA binary duplexes, ternary double triplexes, and tetraplexes. The enhanced stability and augmented molecular recognition properties of the bimodal PNAs can be exploited to design complex supramolecular nanoassemblies with defined functions tailored for various applications in biotechnology as well as material science.[25] Among the probable biological applications, bimodal PNAs can be used to specifically and concurrently target two genes, inhibit micro RNA structures, to probe biological processes and modulate them for therapeutics.[26] Further, bimodal PNAs can used like stapler strands in DNA origami to expand the limits of programmable folding in nucleic acid nanotechnology.[27]

EXPERIMENTAL SECTION

The chemicals used were of laboratory or analytical grade. All the solvents used were distilled or dried to carry out different reactions. Thin layer chromatography (TLC) were used to monitor reactions. Typically, workup involved washing of the organic layer sequentially

with water and brine, drying the organic extract with anhydrous sodium sulphate and subsequent removal of the solvent in roatary evaporator under vacuum. Pre-coated silica gel GF_{254} sheets (Merck 5554) were used for TLC analysis and spots detected under UV illumination, exposure to iodine vapour or by ninhydrin solution spray. Silica gel (60-120 or 100-200 mesh) was used for column chromatographic separations. The PNA oligomers were purified using reverse phase HPLC system equipped with a semipreparative BEH130 C18 (10 X 250 mm) column. The DNA oligonucleotides were obtained commercially from Integrated DNA Technologies (IDT). Salts and reagents used in buffer preparation such as NaCl, sodium cacodylate etc. were obtained from Sigma-Aldrich. The pH of the buffer solutions was adjusted using HCl (Sigma Aldrich). Compounds **6** and **19** were prepared from L-Glutamine by procedure described in reference 17.

^{1}H and ^{13}C NMR spectra were recorded on Bruker AC-400 (400 MHz) or JEOL 400 MHz NMR spectrometers using $CDCl_3$ or DMOSO-d_6 as solvents. The chemical shift values are reported in parts per million (ppm, δ scale) with reference to the internal TMS as standard. The optical rotation were measured on Rudolph Research Analytical Autopol V polarimeter. All UV-Visible spectral measurements were done on Perkin Elmer Lambda 45 double beam spectrometer. The mass spectra of all compounds were obtained by HRMS and the mass of PNA oligomers was confirmed by MALDI-TOF/TOF data using DHB (2,5-Dihydroxybenzoic acid) or CHCA (α-Cyno-4-hydroxycinnamic acid) as matrix.

N-ethylamino(tertbutoxycarbonyl)-N(acetamido-N1-thyminyl)-2(*S*)-[(Fmoc) aminoethyl] glycine (1)

To compound **6** (1 g, 2 mmol) dissolved in ethanol, 10% Pd/C on charcoal was added under H_2 atmosphere and stirred at room temperature for 6 h. After the reaction was complete as monitored by TLC, the reaction mixture was filtered on celite-545 pad and the filtrate evaporated to get solid residue (crude weight 0.8 g). The free amine (1 g, 2 mmol) was dissolved in 10 mL THF:H_2O (1:1) taken in a clean flask and stirred at 0 ºC. Na_2CO_3 (0.5 g, 5 mmol) was added to the reaction mixture followed by slow dropwise addition of Fmoc-Cl (0.6 g, 2 mmol). The reaction mixture was stirred at 0 ºC for 1 h and then at 25 ºC for 4 h. The solvent was evaporated on a rotary evaporator. The residue was dissolved in water (10 mL) and washed with of diethyl ether (20 mL). It was neutralized with 10% aq. HCl and extracted with EtOAc (25 mL × 3). The resisdue obtained after concentration of the combined organic extract was purified by column chromatography to yield compound **1** (1.0 g, 86%). R_f = 0.50

Methanol/DCM (20:80); $[\alpha]D^{25}$= -3.21 (c= 0.5%, MeOH); ^{1}H NMR (400 MHz, DMSO-d_6) δ 11.28 (s, 1H), 7.89-7.87 (d, 2H, J = 8 Hz), 7.68- 7.67 (d, 2H, J = 4 Hz), 7.40 (t, 2H, J = 16 Hz), 7.32 (t, 2H, J = 16 Hz), 7.21 (s, 1H), 7.17 (s, 1H), 4.80-4.46 (m, 2H), 4.31-4.20 (m, 4H), 4.03-3.60 (m, 3H), 3.23-2.97 (m, 4H), 4.03-360 (m, 3H), 3.23-2.97 (m, 4H), 1.74 (maj) 1.72 (min) (S, 2H), 1.37 (maj) 1.35 (min) (s, 9H) ppm. $^{13}C\{^{1}H\}$ NMR (100 MHz, DMSO-d_6) δ 172.0, 170.6, 170.4, 167.9, 167.3, 164.3, 156.1, 155.1, 155.6, 150.1, 143.1, 143.9, 141.9, 141.7, 140.7, 127.6, 127.1, 125.1, 120.1, 108.2, 78.0, 77.8, 66.4, 65.3, 59.8, 47.6, 46.8, 46.3, 39.5, 37.5, 31.9, 28.3, 21.1, 20.8, 14.1, 12 ppm. HRMS (ESI-TOF) m/z calcd for $C_{33}H_{39}N_5O_9$ $[M+Na]^+$ 672.2648, found 672.0918.

5-Amino-2(*R*)-[(tert-butoxycarbonyl)amino]-5-oxopentanoic acid (8)

A solution of di-*tert*-butyl dicarbonate [$(Boc)_2O$] (16.5 g, 17 mL, 75 mmol) in dioxane (100 mL) was added in portion to an ice-cold solution of D-glutamine **7** (10 g, 68 mmol) in aq. NaOH (1 N, 100 mL). The reaction mixture was stirred at 0 °C for 1 h, after which dioxane was completely removed under vacuum. The aqueous layer was washed with diethyl ether to remove excess [$(Boc)_2O$], acidified by addition of saturated aq. $KHSO_4$ to pH 2-3 under cooling and extracted with EtOAc (3 × 150 mL). The combined organic extracts dried over an. Na_2SO_4, was evaporated to obtain compound **8** as a white powder which was used without further purification (14.5 g, 86% yield). HRMS (ES-TOF) *m/z* calcd for $C_{10}H_{18}N_2O_5$ $[M+ H]^+$ 246.1216, found 246.1494.

4-amino-2-(*R*)-[(tert-butoxycarbonyl)amino] butanoic acid (9)

A slurry of compound **8** (5 g, 20 mmol), EtOAc (25 mL), ACN (25 mL), water (12 mL) and iodobenzene diacetate (8 g, 24 mmol) was stirred at 16 °C for 30 min and stirring continued at 20 oC for 4 h. It was filtered under vacuum and the filter cake was washed with EtOAc and dried in vacuum to obtain compound **7** (2.6 g). R_f = 0.2 EtOAc/MeOH (50:50); ^{1}H NMR (400 MHz, DMSO-d_6) 6.18 (1 H, s), 3.61 (2 H, s), 3.02 (2H, d, *J* 7.9), 2.82 – 2.64 (1 H, m), 1.57 – 1.06 (10 H, m). ^{13}C $\{^{1}H\}$ (101 MHz, DMSO-d_6) 171.10, 155.13, 78.17, 50.98, 40.57, 39.52, 31.31, 28.15. HRMS (ESI-TOF) *m/z* calcd for $C_9H_{18}N_2O_4$ $[M + Na]^+$ 218.1267, found 218.1756.

4-amino (benzyloxy)carbonyl)-2(*R*)-[tert-butoxycarbonyl)amino]butanoic acid (10)

To an ice-cold solution of compound **9** (1 g, 4.6 mmol) in acetone (25 mL), aq. $NaHCO_3$ (1 g, 15 mL, 14 mmol) was added and stirred at 0 °C for 10 min. To this, benzylchloroformate

(2 g, 2 mL, 5.5 mmol) in toluene was added and stirring of the reaction mixture was continued overnight at room temperature. The organic solvent was removed under vacuum, the aqueous layer was washed with diethyl ether (2 x 30 mL), acidified with saturated aq. $KHSO_4$ to pH 2-3 and extracted with EtOAc (3 x 60 mL). The combined organic layer was dried and evaporated to give compound **10** as sticky oil (1.45 g, 90% yield). R_f = 0.67 EtOAc/MeOH (50:50). ^{1}H NMR (400 MHz, $CDCl_3$) δ 7.37 – 7.27 (m, 5H), 5.58 (d, *J* = 49.7 Hz, 2H), 5.35 (m, *J* = 40.1 Hz, 1H), 5.14 – 5.02 (m, 2H), 4.40 – 4.28 (m, 1H), 3.71 (s, 2H), 3.54 – 3.41 (m, 1H), 3.14 – 3.00 (m, 1H), 2.07 (d, *J* = 3.9 Hz, 1H), 1.69 (dd, *J* = 9.0, 4.8 Hz, 1H), 1.46 – 1.38 (m, 9H). ^{13}C{^{1}H} NMR (101 MHz, $CDCl_3$) δ 175.0, 173.2, 156.9, 156.6, 136.6, 128.6, 128.2, 80.4, 77.2, 66.8, 52.6, 51.0, 37.2, 33.6, 30.1, 28.4. HRMS (ESI-TOF) *m/z* calcd for $C_{17}H_{24}N_2O_6$ $[M + H]^+$ 353.1713, found 353.1454.

4-amino(benzyloxy)carbonyl)-2(*R*)-[(tert-butoxycarbonyl)amino]methylbutanoate (11)

To a stirred solution of compound **10** (5 g, 15 mmol) and K_2CO_3 (5.0 g, 36 mmol) in acetone (70 mL), dimethyl sulfate (2 mL, 17.5 mmol) (caution: dimethylsulphate is hazardous and must refer to material safety sheet befor handling) was added. The reaction mixture was heated to 55 °C for 5 h under reflux, the solvent was evaporated and to the concentrate, water (90 mL) was added. It was then extracted with EtOAc (3 × 50 mL) and the combined organic layer was washed with brine, dried and concentrated. The residue obtained was purified on column chromatography to give compound **11** as white solid (2.4 g, 93% yield). mp = 65-68 °C; R_f = 0.5 petroleum ether/EtOAc (70:30); ^{1}H NMR (400 MHz, $CDCl_3$) δ 7.38 – 7.28 (m, 5H), 5.50 (s, 1H), 5.26 (s, 1H), 5.10 (q, *J* = 12.3 Hz, 2H), 4.37 (t, *J* = 8.5 Hz, 1H), 3.72 (s, 3H), 3.54 – 3.43 (m, 1H), 3.11 – 3.00 (m, 1H), 2.07 (dd, *J* = 8.4, 4.4 Hz, 1H), 1.89 (s, 1H), 1.73 – 1.62 (m, 1H), 1.43 (s, 9H). ^{13}C{^{1}H} NMR (101 MHz, $CDCl_3$) δ 173.15, 156.5, 156.0, 136.7, 128.6, 128.2, 80.4, 77.2, 66.8, 52.6, 51.0, 37.2, 33.7, 28.4. HRMS (ESI-TOF) *m/z* calcd for $C_{18}H_{26}N_2O_5$ $[M]^+$ 366.4088, found 366.9160.

4-Amino(benzyloxycarbonyl)-2(*R*)-[(tert-butoxycarbonyl)amino]-butanol (12)

To a solution of compound **11** (2.5 g, 13.0 mmol) in absolute EtOH (30 mL) was added $NaBH_4$ (0.6 gm, 20.5 mmol) and stirred for 6 h under N_2 atmosphere at room temperature. After complete removal of ethanol under vaccum, water (60 mL) was added to the concentrate and extracted with EtOAc (3 x 30 mL). The pooled organic extract was washed with brine, dried over anhydrous Na_2SO_4, filtered and concentrated. The residue was purified by column chromatography to give compound **12** as white solid (2.0 g, 89 % yield). M.p = 80-82 °C; R_f =

0.4 petroleum ether/EtOAc (50:50); ^{1}H NMR (400 MHz, DMSO-d_6) δ 7.82 – 7.72 (m, 5H), 6.27 (s, 1H), 5.65 (d, *J* = 8.4 Hz, 1H), 5.53 (q, *J* = 12.3 Hz, 2H), 4.16 – 3.94 (m, 4H), 3.87 (dd, *J* = 12.8, 6.1 Hz, 1H), 3.47 (d, *J* = 5.3 Hz, 1H), 3.04 (s, 8H), 2.22 – 2.10 (m, 1H), 2.08 – 1.96 (m, 1H), 1.93 – 1.83 (m, 9H). ^{13}C{^{1}H} NMR (101 MHz, $CDCl_3$) δ 156.7, 136.8, 128.6, 128.2, 80.0, 77.1, 66.7, 65.6, 49.9, 37.8, 32.3, 28.5. HRMS (ES-TOF) *m/z* calcd for $C_{17}H_{26}N_2O_5$ $[M]^+$, 338.1842, found 338.3427

4-Amino(benzyloxycarbonyl)-2(*R*)-[(tert-butoxycarbonyl)amino]butylmethane sulfonate (13)

To an ice-cold solution of compound **12** (2 g, 6 mmol) in dry DCM (30 mL), triethyl amine (2.0 mL, 15 mmol) and mesyl chloride (0.6 mL, 8 mmol) were added and the mixture was kept stirring for 30 min at 0 ºC under N_2 atmosphere. DCM (30 mL) was added and washed with water (30 mL) and brine (20 mL). The organic layer was dried and concentrated to give compound **13** (2.3 g). R_f = 0.53 petroleum ether/EtOAc (50:50). This compound was used for next step without further purification.

4-Amino(benzyloxy)carbonyl)-2(*R*)-[(tert-butoxycarbonyl)amino]-butylazide (14)

A solution of compound **13** (2.0 g, 5.5 mmol) and sodium azide (5.5 g, 82.5 mmol) in dry DMF (55 mL) was heated for 6 h at 80 ˚C. Water (60 mL) was added, extracted with ethyl acetate (3 x 30 mL) and the combined extract was washed with water (25 mL) followed by brine (25 mL). The dried organic layer was concentrated to obtain a residue that was purified by column chromatography to give compound **14** as sticky yellowish oil (1.4 g, 80% yield). R_f = 0.73 petroleum ether/EtOAc (50:50); ^{1}H NMR (400 MHz, $CDCl_3$) δ 7.44 – 7.30 (m, 31H), 5.47 (s, 1H), 5.11 (q, *J* = 12.3 Hz, 2H), 4.73 (s, 1H), 3.84 (s, 1H), 3.45 (d, *J* = 16.0 Hz, 3H), 3.08 – 2.96 (m, 1H), 1.74 (dd, *J* = 8.3, 4.3 Hz, 1H), 1.59 (dt, *J* = 13.7, 7.2 Hz, 1H), 1.46 (s, 9H). ^{13}C{^{1}H}NMR (101 MHz, $CDCl_3$) δ 156.5, 155.9, 136.6, 128.5, 128.1, 80.1, 66.7, 55.2, 47.7, 37.5, 33.1, 28.3. HRMS (ESI-TOF) *m/z* calcd. for $C_{17}H_{25}N_5O_4$ $[M]^+$, 363.1907, found 363.2510

N-ethylamino-(tert-butoxycarbonyl)amino)-2(*R*)-[(benzyloxycarbonyl)amino]ethyl glycinate (15)

A solution of compound **14** (0.7 mg, 2.0 mmol) in absolute EtOH (15 mL) taken in hydrogenation flask (Parr reactor) was mixed with Raney Nickel (2 mL). It was hydrogenated with H_2 pressure of 50-55 psi for 6 h at room temperature . The catalyst was filtered off from

reaction mixture, and the filtrate was concentrated to yield a residual yellowish oil of amine (630 mg, 1.8 mmol). This was treated with ethylbromo acetate (0.2 mL, 1.7 mmol) and triethyl amine (0.8 mL) in ACN (20 mL) and the reaction mixture was stirred at room temperature for 12 h. The solvent was evaporated under vacuum, water (50 mL) was added to the concentrate and The aqueous layer was extracted with EtOAc (3 × 40 mL). The combined organic extract was washed with sat. $NaHCO_3$ followed by brine, dried and concentrated on rotary evaporator. The residue obtained was purified on silica gel (100-200 mesh) using petroleum ether and ethyl acetate to give compound **15** as yellowish oil (0.65 mg, 80%). R_f = 0.48 petroleum ether/EtOAc (20:80); ^{1}H NMR (400 MHz, $CDCl_3$) δ 7.40 – 7.31 (m, 5H), 5.61 (s, 1H), 5.05 (ddd, *J* = 26.6, 19.7, 9.8 Hz, 4H), 4.24 – 4.14 (m, 3H), 4.03 (s, 1H), 3.98 – 3.67 (m, 2H), 3.50 (ddd, *J* = 21.0, 18.4, 6.3 Hz, 2H), 3.17 (d, *J* = 10.4 Hz, 1H), 3.10 – 2.99 (m, 1H), 1.90 – 1.65 (m, 2H), 1.42 (s, 9H), 1.32 – 1.27 (m, 3H). ^{13}C{^{1}H} NMR (101 MHz, $CDCl_3$) δ 168.9, 168.6, 156.7, 136.8, 136.6, 128.6, 128.3, 79.8, 77.2, 66.7, 61.7, 53.1, 51.0, 50.0, 49.0, 47.5, 47.2, 41.0, 40.8, 37.8, 33.6, 32.8, 28.5, 14.2. HRMS (ESI-TOF**)** *m/z* calcd for $C_{21}H_{33}N_3O_6$ $[M]^+$ 423.2369, found 423.0408.

N-ethylamino(tertbutoxycarbonyl)-N(chloroacetamido)-2(*R*)-[(benzyloxycarbonyl) aminoethyl] ethyl glycinate (16)

To an ice-cold solution of compound **15** (3.0 g, 7.3 mmol) and triethyl amine (3 g; 4 mL, 30 mmol) in dry DCM (50 mL) was treated with chloroacetyl chloride (0.6 mL, 7.3 mmol) and the reaction mixture was stirred for 8 h. DCM (20 mL) was added to the reaction mixture and washed with water (50 mL) and brine (50 mL). The dried organic extract was concentrated and the residue was purified on silica gel (100-200 mesh) using petroleum ether and EtOAc to give compound **16** as colourless sticky oil (2.5 g, 72 %). R_f = 0.59 petroleum ether/EtOAc (40:60); ^{1}H NMR (400 MHz, $CDCl_3$) δ 7.33 (dt, *J* = 8.3, 4.0 Hz, 5H), 5.08 (q, *J* = 12.8 Hz, 2H), 4.41 (dd, *J* = 39.3, 16.3 Hz, 2H), 4.30 – 4.08 (m, 4H), 3.86 – 3.61 (m, 2H), 3.37 (dd, *J* = 46.5, 9.9 Hz, 2H), 3.20 – 2.85 (m, 4H), 2.05 (d, *J* = 9.5 Hz, 2H), 1.91 – 1.88 (m, 2H), 1.40 (d, *J* = 8.1 Hz, 9H), 1.25 (t, *J* = 7.1 Hz, 3H). ^{13}C{^{1}H} NMR (101 MHz, $CDCl_3$) δ 169.2, 168.6, 167.6, 164.4, 156.9, 151.5, 141.0, 136.8, 128.6, 128.2, 111.0, 79.9, 77.2, 62.5, 61.7, 60.5, 52.4, 51.7, 50.0, 47.9, 37.9, 33.2, 32.5, 28.5, 14.3, 12.4. HRMS (ESI-TOF) *m/z* calcd for $C_{23}H_{34}ClN_3O_6$ $[M]^+$ 499.2085, found 499.1733.

N-ethylamino(tertbutoxycarbonyl)-N(acetamido-N1-thyminyl)-2(*R*)-[(benzyloxy carbonyl) aminoethyl] ethyl glycinate (17)

A solution of compound **16** (1 g, 2 mmol), K_2CO_3 (0.3 g, 2.5 mmol) and thymine (0.3 g, 2.5 mmol) in dry DMF (20 mL) was stirred at room temperature for 12 h. Water (50 mL) was added to the reaction mixture and product was extracted into EtOAc (3 x 40 mL). The organic layer after work up was dried and concentrated to yield a residue which was purified on silica gel (100-200 mesh) using petroleum ether and ethyl acetate to give compound **17** as white solid (0.97 g, 88%); R_f = 0.47 EtOAc (100); ^{1}H NMR (400 MHz, $CDCl_3$) δ 9.70 (d, *J* = 120.7 Hz, 1H), 7.35 – 7.27 (m, 5H), 7.00 (d, *J* = 26.8 Hz, 1H), 5.70 – 5.51 (m, 1H), 5.06 (q, *J* = 12.5 Hz, 2H), 4.79 (d, *J* = 16.2 Hz, 1H), 4.47 – 4.32 (m, 1H), 4.30 – 4.08 (m, 4H), 3.91 (d, *J* = 17.2 Hz, 1H), 3.76 (d, *J* = 41.0 Hz, 1H), 3.65 – 3.48 (m, 2H), 3.47 – 3.26 (m, 1H), 3.06 (ddd, *J* = 19.7, 14.2, 6.1 Hz, 3H), 2.15 (s, 1H), 1.87 (d, *J* = 7.2 Hz, 3H), 1.73 – 1.58 (m, 1H), 1.39 (d, *J* = 9.8 Hz, 9H), 1.26 (dt, *J* = 21.1, 7.1 Hz, 3H). ^{13}C{^{1}H} NMR (101 MHz, $CDCl_3$) δ 169.3, 168.6, 167.6, 164.5, 156.8, 156.2, 151.6, 151.3, 141.3, 136.7, 128.5, 128.1, 111.0, 80.0, 79.8, 66.7, 62.4, 61.6, 52.2, 51.6, 49.9, 48.7, 47.9, 47.3, 37.9, 37.6, 33.0, 32.3, 28.4, 14.2, 12.4 ppm. HRMS (ESI-TOF) *m/z* calcd for $C_{28}H_{39}N_5O_9$ $[M + Na]^+$ 612.2748,found 612.2722

N-ethylamino(tertbutoxycarbonyl)-N(acetamido-N1-thyminyl)-2(*S*)-[(benzyloxy carbonyl) aminoethyl] glycine (18)

To a stirred solution of compound **17** (0.5g, 1 mmol) in MeOH was added 10% aq. LiOH and reaction mixture was stirred at room temperature for 3-4 h. The solvent was removed under vacuum and the aqueous layer was neutralized with activated Dowex H^+ resin till pH of the solution reached 5.0. The resin was filtered out and the filtrate was concentrated to obtain compound **18** as white solid (0.4 g, 85%). M.p = 241-245 °C; R_f = 0.5 EtOAc/MeOH (50:50); ^{1}H NMR (400 MHz, $CDCl_3$) δ 7.78 (d, *J* = 8.4 Hz, 2H), 7.66 – 7.50 (m, 2H), 7.35 (dd, *J* = 28.0, 8.6 Hz, 4H), 5.55 – 5.10 (m, 1H), 4.65 – 4.32 (m, 2H), 4.22 (s, 1H), 3.96 (d, *J* = 14.0 Hz, 1H), 3.64 (d, *J* = 72.1 Hz, 1H), 3.11 (s, 1H), 2.78 (d, *J* = 46.7 Hz, 1H), 2.08 – 1.86 (m, 1H), 1.84 – 1.61 (m, 2H), 1.46 (dd, *J* = 16.2, 4.8 Hz, 9H). ^{13}C{^{1}H} NMR (101 MHz, DMSO-d_6) δ 172.3, 170.8, 168.1, 167.5, 164.5, 156.2, 155.8, 151.0, 142.0, 137.4, 128.6, 128.0, 108.5, 78.3, 65.4, 51.3, 48.8, 47.9, 46.6, 39.5, 37.9, 32.0, 28.4, 21.3, 12.2 ppm. HRMS (ESI-TOF) *m/z* calcd for $C_{26}H_{35}N_5O_9$ $[M]^+$ 561.2435, found 561.2143.

N-ethylamino(tertbutoxycarbonyl)-N(acetamido-N1-thyminyl)-2*S*-[(Fmoc) aminoethyl] glycine (2)

Compound **18** (1 g, 2 mmol) was dissolved in ethanol containing 10% Pd/C and subjected to H_2 atmosphere in a ballon with stirring at room temperature for 6 h. After the

reaction was complete as monitored by TLC, it was filtered on celite-545 pad and the filtrate was evaporated to get solid product (crude weight 0.8 g). The free amine was dissolved in THF:H_2O (1:1, 10 mL) in a flask, stirred with solid Na_2CO_3 (0.5 g, 5 mmol) at 0 ºC, followed by dropwise addition of Fmoc-Cl (0.6 g, 2 mmol). After 1 h at 0ºC, temp was raised to 25 ºC and kept for 3 h. The reaction mixture was concentrated on a rotary evaporator and the residue was dissolved in water (10 mL) and washed with of diethyl ether (20 mL). After neutralization with 10% HCl, it was extracted with EtOAc (25 mL × 3) and the dried organic layer on concentration gave a residue that was purified by column chromatography to yield compound **2** (1.0 g, 86%). R_f = 0.50 Methanol/DCM (20:80); $[\alpha]D^{25}$= + 3.19 (c= 0.5% , MeOH); ^{1}H NMR (400 MHz, DMSO-d_6) δ 12.58 (s, 1H), 11.28 (d, *J* = 3.0 Hz, 1H), 7.88 (d, *J* = 7.5 Hz, 2H), 7.68 (d, *J* = 6.5 Hz, 2H), 7.41 (t, *J* = 7.4 Hz, 2H), 7.36 – 7.27 (m, 2H), 7.23 – 7.14 (m, 1H), 6.79 (dd, *J* = 66.5, 9.0 Hz, 1H), 4.58 (ddd, *J* = 46.1, 28.4, 12.1 Hz, 2H), 4.37 – 4.12 (m, 3H), 3.98 (dt, *J* = 39.4, 12.3 Hz, 1H), 3.51 – 3.15 (m, 4H), 3.05 (ddd, *J* = 18.4, 13.5, 8.0 Hz, 2H), 1.95 (d, *J* = 30.2 Hz, 1H), 1.77 – 1.69 (m, 2H), 1.37 (d, *J* = 10.7 Hz, 9H), 1.17 (t, *J* = 7.1 Hz, 1H). ^{13}C{^{1}H} NMR (101 MHz, DMSO-d_6) δ 172.0, 170.6, 167.9, 167.3, 164.3, 156.1, 155.1, 155.6, 150.1, 143.1, 143.9, 141.7, 140.7, 127.6, 127.1, 125.1, 120.1, 108.2, 78.0, 77.8, 66.4, 65.3, 59.8, 47.6, 46.8, 39.5, 37.5, 31.9, 28.3, 21.1, 20.8, 14.1, 12 ppm. HRMS (ESI-TOF) m/z calcd. for $C_{33}H_{39}N_5O_9$ $[M]^+$ 649.2748, found 649.2596

N(Acetyl)-N-ethylamino(tertbutoxycarbonyl)-2(*S*)-[(benzyloxycarbonyl)aminoethyl] ethyl glycinate (20)

To a stirred solution of **19** (1 g, 2.5 mmol) in dry DCM (10 mL) was added DCC (0.7 g, 4 mmol) and DhbtOH (0.6 g, 4 mmol) and the reaction mixture was stirred at room temperature for 10 min. Glacial acetic acid (0.2 mL, 4 mmol) was added and stirring continued overnight. Removal of solvent under reduced pressure gave a residue which was dissolved in EtOAc (300 mL), washed with saturated aq. $NaHCO_3$ (300 mL) followed by aq. $KHSO_4$ (10%, 300 mL). After usual work up, the organic layer was concentrated under reduced pressure to obtain crude product that was purified by column chromatography to afford compound **20** (1.5 gm, 80%) as a sticky oil. ^{1}H NMR (400 MHz, $CDCl_3$) δ 7.37 – 7.27 (m, 5H), 5.63 (s, 1H), 5.13 – 5.03 (m, 2H), 4.27 – 4.10 (m, 3H), 4.08 – 3.96 (m, 2H), 3.88 (d, *J* = 17.1 Hz, 3H), 3.82 – 3.62 (m, H), 3.51 – 3.35 (m, 2H), 3.17 – 2.83 (m, 2H), 2.07 (d, *J* = 41.0 Hz, 3H), 1.91 – 1.55 (m, 3H), 1.40 (d, *J* = 4.9 Hz, 9H), 1.26 (dt, *J* = 11.2, 7.1 Hz, 3H). ^{13}C{^{1}H} NMR (101 MHz, $CDCl_3$) δ 172.6, 171.5, 170.1, 169.2, 156.8, 136.8, 128.6, 128.1, 80.1, 79.6, 77.2, 66.6, 61.9,

61.5, 51.0, 50.5, 47.4, 37.9, 37.6, 33.5, 32.6, 28.5, 21.5, 14.2 ppm. HRMS (ESI-TOF) m/z calcd. for $C_{23}H_{35}N_3O_7$ $[M]^+$ 465.2475, found 465.1733.

N-ethylamino(tertbutoxycarbonyl)-N(acetamido-N1-thyminyl)-2(*S*)-[(benzyloxy carbonyl) aminoethyl] ethyl glycine (21)[17]

A solution of compound **20** (0.5g, 1 mmol) in MeOH was treated with 10% aq. LiOH and reaction mixture was stirred at room temperature for 3-4 h. The solvent was removed under vacuum and the aqueous layer was washed with diethyl ether. It was neutralized with activated Dowex H^+ resin till pH of the solution reached 5.5, The resin was removed by filtration and the filtrate concentrated to obtain compound **21** as white solid (0.4 g, 85%); R_f = 0.5 EtOAc/MeOH (50:50); ^{1}H NMR (400 MHz, $CDCl_3$) δ 7.38 – 7.28 (m, 5H), 5.50 (d, *J* = 89.1 Hz, 1H), 5.13 – 5.03 (m, 2H), 4.18 – 3.92 (m, 3H), 3.75 (t, *J* = 23.4 Hz, 2H), 3.46 (ddd, *J* = 34.8, 10.5, 7.1 Hz, 2H), 3.09 (dd, *J* = 28.3, 9.8 Hz, 1H), 2.17 – 2.02 (m, 3H), 1.83 – 1.60 (m, 2H), 1.38 (dd, *J* = 17.1, 6.5 Hz, 9H). ^{13}C NMR (101 MHz, $CDCl_3$) δ 173.0, 171.3, 157.0, 136.3, 128.3, 77.2, 66.7, 50.3, 47.7, 37.5, 29.7, 28.2, 21.4,20.8 ppm. HRMS (ESI-TOF) *m/z* calcd for $C_{21}H_{31}N_3O_7$ $[M + K]^+$. 476.1799, found 476.0979.

N(Acetyl)-N-ethylamino(tertbutoxycarbonyl)-2(*S*)-[(Fmoc)aminoethyl] glycine (3)

To compound **21** (1 g, 2 mmol) dissolved in EtOH, 10% Pd/C on charcoal was added under H_2 atmosphere and stirred at room temperature for 6 h, when the reaction got completed as monitored by TLC. The charcoal was filtered on celite-545 pad and filtrate was evaporated to get solid product (0.8 g) which was dissolved in 10 mL THF:H_2O (1:1). It was stirred at 0 ºC with Na_2CO_3 (0.5 g, 5 mmol) followed by dropwise addition of Fmoc-Cl (0.6 g, 2 mmol). The stirring was continued at 0 ºC for 1 h and then at 25 ºC for 3 h to complete the reaction. Evaporation of solvent gave a residue that was dissolved in water (10 mL) and washed with diethyl ether (20 mL). It was then neutralised with 10% aq. HCl and extracted with EtOAc (25 mL×3). The organic layer upon concentration gave a residue that was purified by column chromatography to yield compound **3** (1.0 g, 70 %). ^{1}H NMR (400 MHz, $CDCl_3$) δ 7.74 (d, *J* = 7.5 Hz, 2H), 7.64 – 7.50 (m, 2H), 7.38 (t, *J* = 7.4 Hz, 2H), 4.81 – 4.28 (m, 7H), 4.24 – 3.89 (m, 1H), 3.84 – 3.63 (m, 2H), 3.55 – 3.28 (m, 5H), 3.27 – 2.87 (m, 6H), 2.19 – 1.98 (m, 3H), 1.82 – 1.47 (m, 2H), 1.36 (t, *J* = 32.1 Hz, 9H**)**. ^{13}C{^{1}H} NMR (101 MHz, $CDCl_3$) δ 175.4, 141.1, 127.5, 126.9, 119.7, 77.2, 47.1, 28.1, 20.4 ppm. HRMS (ESI-TOF) m/z calcd. for $C_{28}H_{35}N_3O_7$ $[M +K]^+$ 564.2112, found 564.0740.

N(Acetyl)-N-ethylamino(tertbutoxycarbonyl)-2(*R*)-[(benzyloxycarbonyl)aminoethyl] ethyl glycinate (22)

A stirred solution of **15** (1 g, 2.5 mmol) in dry DCM (10 mL) was treated with DCC (0.7 g, 4 mmol) and DhbtOH (0.6 g, 4 mmol). The resulting mixture was stirred at room temperature for 10 min after which glacial acetic acid (0.2 mL, 4 mmol) was added and the stirring continued for overnight. The organic solvent was removed under reduced pressure, to yield a residue that was dissolved in EtOAc (300 mL), followed by aqueous work up and concentration of organic extract gave a residue which was purified by column chromatography to afford **22** (1.5 gm, 85%) as a sticky oil. ^{1}H NMR (400 MHz, $CDCl_3$) δ 7.37 – 7.27 (m, 5H), 5.63 (s, 1H), 5.13 – 5.03 (m, 2H), 4.27 – 4.10 (m, 3H), 4.08 – 3.96 (m, 2H), 3.88 (d, *J* = 17.1 Hz, 3H), 3.82 – 3.62 (m, H), 3.51 – 3.35 (m, 2H), 3.17 – 2.83 (m, 2H), 2.07 (d, *J* = 41.0 Hz, 3H), 1.91 – 1.55 (m, 3H), 1.40 (d, *J* = 4.9 Hz, 9H), 1.26 (dt, *J* = 11.2, 7.1 Hz, 3H). ^{13}C{^{1}H} NMR (101 MHz, $CDCl_3$) δ 172.6, 171.5, 170.1, 169.2, 156.8, 136.8, 128.6, 128.1, 80.1, 79.6, 77.2, 66.6, 61.9, 61.5, 51.0, 50.5, 47.4, 37.9, 37.6, 33.5, 32.6, 28.5, 21.5, 14.2 ppm. HRMS (ESI-TOF) m/z calcd. for $C_{23}H_{35}N_3O_7$ $[M+H]^+$ 466.2553, found 466.3684.

N(Acetyl)-N-ethylamino(tertbutoxycarbonyl)-2(*R*)-[(benzyloxycarbonyl) aminoethyl] glycine (23)

To a stirred solution of compound **22** (0.70 g, 1.5 mmol) in THF (15 mL), aq. NaOH (2 M, 15 mL) was added at 0 °C and kept stirred for 1 hr at 0 °C. Water (50 mL) was added, and the resulting mixture was extracted with EtOAc (2 × 35 mL). The aqueous layer containing the product was neutralized with saturated aq. $KHSO_4$ at 0 °C to pH 3−4 and extracted into EtOAc (4 x 35 mL). The combined organic extracts after drying and concentration gave crude product that was purified by column chromatography to afford **23** as a white solid (0.63 g, 90%). ^{1}H NMR (400 MHz, $CDCl_3$) δ 7.31 (dt, *J* = 12.0, 4.1 Hz, 5H), 5.09 (t, *J* = 9.6 Hz, 2H), 4.21 – 3.86 (m, 2H), 3.74 (t, *J* = 18.5 Hz, 5H), 3.44 (d, *J* = 32.9 Hz, 1H), 3.17 – 3.00 (m, 8H), 2.15 – 2.02 (m, 3H), 1.84 – 1.54 (m, 2H), 1.48 – 1.34 (m, 9H). ^{13}C{^{1}H} NMR (101 MHz, $CDCl_3$) δ 173.0, 171.3, 157.0, 136.3, 128.3, 77.2, 66.7, 50.3, 47.7, 37.5, 29.8, 28.2, 21.4, 20.8 ppm. HRMS (ESI-TOF) m/z calcd. for $C_{20}H_{29}N_3O_7$ $[M+Na]^+$ 460.2060, found 460.2320.

N(Acetyl)-N-ethylamino(tertbutoxycarbonyl)-2(*R*)-[(Fmoc)aminoethyl] glycine (4)

To the compound **23** (1 g, 2 mmol) dissolved in ethanol, 10% Pd/C on charcoal was added under H_2 atmosphere and stirred at room temperature for 6 h. after which it was filtered on celite-545 pad. The filtrate was evaporated to get crude amine product (crude weight 0.8 g)

which was dissolved in 10 mL THF:H_2O (1:1), stirred at 0 ºC with Na_2CO_3 (0.5 g, 5 mmol). followed by dropwise addition of Fmoc-Cl (0.6 g, 2 mmol). The reaction mixture was kept stirred at 0 ºC for 1 h and then at 25 ºC for 3 h. after which solvent was evaporated and the residue was dissolved in of water (10 mL) and washed with diethyl ether (20 ml). After neutralization with with 10% aq. HCl, product was extracted with ethyl acetate (25 mL × 3), the dried organic layer was concentrated to obtain a residue obtained that was purified by column chromatography to yield compound **4** (1.0 g, 66 %). ^{1}H NMR (400 MHz, $CDCl_3$) δ 7.74 (d, *J* = 7.5 Hz, 2H), 7.64 – 7.50 (m, 2H), 7.38 (t, *J* = 7.4 Hz, 2H), 4.81 – 4.28 (m, 7H), 4.24 – 3.89 (m, 1H), 3.84 – 3.63 (m, 2H), 3.55 – 3.28 (m, 5H), 3.27 – 2.87 (m, 6H), 2.19 – 1.98 (m, 3H), 1.82 – 1.47 (m, 2H), 1.36 (t, *J* = 32.1 Hz, 9H**)**. ^{13}C{^{1}H} NMR (101 MHz, $CDCl_3$) δ 175.4, 141.1, 127.5, 126.9, 119.7, 77.2, 47.1, 28.1, 20.4 ppm. HRMS (ESI-TOF) m/z calcd. for $C_{28}H_{35}N_3O_7$ $[M+K]^+$ 564.2112, found 564.2699.

Solid-Phase Synthesis

The PNA oligomers were synthesized on MBHA (4-methyl–benzhydryl amine) resin using combination of Boc and Fmoc protocols.[27] The solid-phase synthesis was carried out in a reactor with a sintered glass bottom, using MBHA resin with loading value of 0.20 mmol/g. The deprotected NH_2 group on resin was treated with N,N'-protected lysine acid, activated with the coupling reagent mixture of HOBt (6 mg, 3 eq), HBTt (6 mg, 3 eq), DIPEA (10 µL) in DMF. The terminal N-t-Boc group of lysine on resin was first deprotected with 50% TFA in DCM (3 × 15 min) followed by washing with DCM and DMF (3 × 10 mL) to give the TFA salt of amine. This was neutralized using 10% N,N-diisopropylethylamine (DIPEA) in DCM (3 × 10 min) to liberate free amine on resin. The resin was then coupled with activated carboxylic acid group of C-*aeg*-PNA monomer using same coupling reagents. The deprotection of NHBoc of *aeg*-C monomer on the resin with TFE was followed by reaction with the incoming Cγ-bimodal monomer **1** using (i) HOBt (3 eq), HBTU (3 eq), DIPEA (3eq) in DMF (Scheme 3) The deprotection of sidechain NHFmoc group after coupling was done using 20% piperidine in DMF followed by side chain coupling with appropriate nucleobase acetic acid (A/T/C; 3 eq) done using HOBt (3 eq), HBTU (3 eq), and DIPEA (3 eq) in DMF (500 µL). After ecery coupling and deprotection step, the resin was successively washed with DCM and DMF (3 x 1 mL) before the next reaction. These cycles were repeated as in Scheme 3 to reach the desired PNA oligomer sequence.

Cleavage of the *bm*-PNA oligomers from solid support

The MBHA resin (10 mg) after complete assembly of Cγ-*bm*-PNA oligomers was stirred with thioanisole (20 μL) and 1,2-ethanedithiol (8 μL) in an ice bath for 10 min. Cold TFA (200 μL) and TFMSA (16 μL) were then added and the reaction mixture with resin was kept stirred for further 1.5 to 2 h at room temperature. The resin was filtered out and washed twice with TFA and the filtrate was concentrated in a microfuge tube and treated with cold diethyl ether to precipitate the PNA prodcut. Upon centrifugation, the sediment was dissolved in 40% $MeNH_2$ solution for deprotection of the isobutyryl group on 2-NH_2 of G nucleobase at rt for 8 h. It was then concentrated on Speedvac for purification by HPLC.

The purification of PNAs was carried out on Agilent HPLC system with semi-preparative BEH130 C18 (10×250 mm) Phenomenex column using solvents water and acetonitrile with composition A: 0.1% TFA in CH_3CN:H_2O (5:95) and B= 0.1% TFA in CH_3CN:H_2O (1:1). The gradient for elution was 100% A to 100% B in 20 min, with flow rate of 2 mL/min. The HPLC elutions were monitored at 220 and 254 nm wavelength.

Temperature-UV absorbance measurements

The temperature dependent UV-absorbance experiments were carried out on Varian Cary 300 UV spectrophotometer equipped with a Peltier heating system. Sodium cacodylate buffer (10 mM, pH 7.2) containing NaCl (10 mM) was used for preparing the samples. The respective PNA and DNA complementary sequences in stoichiometric ratio (1:1, duplex) were mixed to achieve a final concentration of 2 μM for each strand. The samples were heated to 90 °C for and maintained at 10 min. followed by slow cooling over 8-10 h to room temperature. The samples were refrigerated for 24 h and for the experiments 500 μL of sample was transferred to quartz cell and equilibrated at the starting temperature for 5 min. The absorbance at 260 nm was recorded from 20-90 °C with temperature gradient of 0.5 °C/min. The melting experiments were repeated thrice to get consistent values. The normalized absorbance at 260 nm was plotted as a function of the temperature. The data were fitted by sigmoidal curve, function - Boltzmann for one face and biphasic dose response for two face binding, where R square value in range of 0.96 to 0.99. The T_m values were obtained from the peak in first derivative plot of normalized absorbance with respect to temperature and are accurate to ± 1.0 °C. The data were processed using OriginPro 8.5. The concentration of all oligonucleotides were calculated on the basis of UV absorbance at 260 nm from the molar extinction coefficients of the corresponding nucleobases: T = 8.8 cm^2/μmol; C = 6.6 cm^2/μmol; G = 11.7 cm^2/μmol and A = 13.7 cm^2/μmol as per literature.[28]

Circular dichroism spectra

CD spectra were recorded at a temperature 10 °C on a JASCO J-815 spectropolarimeter, with accumulation of 3 scans from 300 to 200 nm using 2 mm cell, a resolution of 0.1 nm, band-width of 1 nm, sensitivity of 2 mdeg, response of 2 sec and a scan speed of 50 nm/min. The calculated amounts of *bm*-PNA oligomers and the complementary DNA were mixed together in stoichiometric ratio (1:1 for duplex) in sodium cacodylate buffer (10 mM) containing and NaCl (10 mM), pH 7.2 to achieve a final strand concentration of 10 μM for each strand. The samples were annealed as in UV-T experiments.

ASSOCIATED CONTENT

Supporting Information: The Supporting Information is available free of charge. Schemes for synthesis of known compounds, ^{1}H and ^{13}C NMR spectra of all new synthetic compounds and key intermediates, HRMS of new compounds, HPLC and MALDI-TOF spectral data of all PNA oligomers

AUTHOR INFORMATION

Corresponding Author

Krishna N Ganesh, Indian Institute of Science Education and Research, Karkambadi Road, Mangalam, Tirupati 517507, India. orcid.org/0000-0003-2292-643X, Email: kn.ganesh@iisertirupati.ac.in

Authors contributions

P. B., Chemical synthesis and Biophysical studies, Indian Institute of Science Education and Research (IISER) Pune, Dr Homi Bhabha Road, Pune 411008. pramod.bhingardeve@students.iiserpune.ac.in

B.M. Contributed to interpretation of UV-melting results, Department of Chemistry, Indian Institute of Science Education and Research (IISER) Tirupati, Tirupati 517507, India; orcid.org/0000-0003-1043-8754 250

Acknowledgements

PB thanks IISER Pune for a research fellowship, BM is a recipient of Post-doctoral fellowshiptp from IISER Tirupati and KNG acknowledges DST, New Delhi, Govt of India for a research grant (EMR/2016/007601).

REFERENCES

1. Nielsen, P. E.; Egholm, M.; Berg, R. H.; Buchardt, O. Sequence selective recognition of DNA by strand displacement with thymine-substituted polyamide, *Science* **1991***, 254*, 1497–1500.

2. Egholm, M.; Buchardt, O.; Nielsen, P. E.; Berg, R. H. Peptide Nucleic Acids (PNA). Oligonucleotide analogues with an achiral peptide backbone. *J. Am. Chem. Soc*. **1992**, *114*, 1895–1897.

3. Egholm, M.; Nielsen, P. E.; Buchardt, O.; Berg, R. H. *J.* Recognition of guanine and adenine in DNA by cytosine and thymine containing peptide nucleic acids (PNA), *J. Am. Chem. Soc*. **1992**, *114*, 9677–9678.

4. Egholm, M.; Buchardt, O; Christensen, L.; Behrens, C.; Freier, S. M.; Driver, D. A.; Berg, R. H.; Kim, S. K.; Norden, B.; Nielsen, P. E. PNA hybridizes to complementary oligonucleotides obeying the Watson–Crick hydrogen-bonding rules, *Nature* **1993**, *365*, 566–568.

5. (a) Nielsen, P. E.; Christensen, L. Strand displacement binding of a duplex forming homopurine PNA to a homopyrimidine duplex DNA target. *J. Am. Chem. Soc*. **1996**, *118*, 2287–2288. (b) Demidov, V. V.; Yavnilovich, M. V.; Belotserkovskii, B. P.; Frank-Kamenetskii, M. D.; Nielsen, P. E. Kinetics and mechanism of polyamide 'peptide' nucleic acid binding to duplex DNA, *Proc. Natl. Acad. Sci. U. S. A.* **1995,** *92,* 2637–2641.

6. (a) Ray, A.; Norden, B. Peptide nucleic acid (PNA): its medical and biotechnical applications and promise for the future, FASEB J. **2000**, *14*, 1041–1060. (b) Nielsen, P. E. PNA technology, *Mol. Biotechnol.* **2004**, *26*, 233–248. (c) Lundin, K. E.; Good, L.; Stromberg, R.; Graslund, A.; Smith, C. I. E. Biological activity and biotechnological aspects of peptide nucleic acid, *Adv. Genet*. **2006**, *56*, 1−51. (d) D'Agata, R.; Giuffrida, M. C.; Spoto, G. Peptide nucleic acid-based biosensors for cancer diagnosis, *Molecules* **2017**, *22*, 1951-1966. (e) Vilaivan, T. Fluorogenic PNA probes, *Beilstein J. Org. Chem.* **2018**, *14*, 253–281. (f) Saarbach, J.; Sabale, P. M.; Winssinger, N. Peptide nucleic acid (PNA) and its applications in chemical biology, diagnostics and therapeutics, *Curr. Opin. Chem. Biol.* **2019**, *52*, 112–124. (g) Economos, N. G.; Oyaghire, S.; Quijano, E.; Adele S. Ricciardi, A. S.; Saltzman, W. M.; Glazer, P. M. Peptide nucleic acids and gene editing: Perspectives on structure and repair, *Molecules* **2020**, *25*, 735–736.

7. (a) Good, L.; Nielsen, P. E.; Progress in developing PNA as a gene-targeted drug, *Antisense Nucleic Acid Drug Dev*. **1997**, *7*, 431–437. (b) Doyle, D. F.; Braasch, D. A.; Janowski, B. A.; Corey, D. R. Inhibition of gene expression inside cells by peptide nucleic acids: Effect of mRNA target sequence, mismatched bases, and PNA length, *Biochemistry* **2001**, *40*, 53–64. (c) Quijano, E.; Bahal, B.; Ricciard, A.; Saltzman, W. M.; Glazer, P. M. Therapeutic peptide nucleic acids: Principles, limitations, and opportunities, *Yale J. Biol. Med*. **2017***, 90,* 583-598. (d) Montazersaheb, S.; Saeid Hejazi, M.; Charoudeh, H. N.; Potential of Peptide nucleic acids in future therapeutic applications, *Adv. Pharm. Bull*. **2018**, *8*, 551–563. (e) Lee, H. T.; Kim, S. K.; Yoon, J. W. Antisense peptide nucleic acids as a potential anti-infective agent, *J. Microbiol*. **2019**, *57*, 423–430 (f) *Gambari, R.; Gasparello, J.; Finotti, A*. Peptide nucleic acid-based targeting of microRNAs: possible therapeutic applications for glioblastoma, *J. Cancer Metastas. Treat.* **2019**, *5*, 55–62. (g) Smith, C. I. E.; Zain, R. Therapeutic oligonucleotides: State of the art, *Annu. Rev. Pharmacol. Toxicol.* **2019**, *59*, 605–630.

8 (a) Hyrup, B.; Egholm, M.; Nielsen, P. E.; Wittung, P.; Norden, B.; Buchardt, O. Structure-Activity studies of the binding of modified peptide nucleic acids (PNAs) to DNA, *J. Am. Chem. Soc*. **1994**, *116*, 7964–7970. (b) Kumar, V. A.; Ganesh, K. N. Conformationally constrained PNA analogues: Structural evolution toward DNA/RNA binding selectivity *Acc. Chem. Res*. **2005**, *38*, 404–412. (c). Govindaraju, T.; Kumar, V. A.; Ganesh, K. N. (*SR*/*RS*)-Cyclohexanyl PNAs: Conformationally preorganized PNA analogues with unprecedented preference for duplex formation with RNA, *J. Am. Chem. Soc*. **2005**, *127*, 4144–4155. (d). Kumar, V. A.; Ganesh, K. N. Structure-editing of nucleic acids for selective targeting of RNA, *Curr. Top. Med. Chem.* **2007**, *7*, 715–726 (e) Corradini, R.; Sforza S.; Tedeschi, T.; Totsingan, F.; Manicardi, A.; Marchelli, R. Peptide nucleic acids with a structurally biased backbone. Updated review and emerging challenges, *Curr. Top. Med. Chem*. **2011**, *11*, 1535–1554. (f) Moccia, M.; Adamo, M. F. A.; Saviano, M. Insights on chiral, backbone modified peptide nucleic acids: Properties and biological activity. *Artif. DNA PNA XNA* **2014**, *5*, e1107176.

9. (a) Koppelhus, U.; Nielsen, P. E. Cellular delivery of peptide nucleic acid (PNA). *Adv. Drug Del. Rev.* **2003**, *55*, 267–280. (b) Równicki, M.; Wojciechowska, M.; Wierzba, A. J.; Czarnecki, J.; Bartosik, D.; Gryko, D.; Trylska, J. Vitamin B12 as a carrier of peptide nucleic acid (PNA) into bacterial cells. *Sci. Rep*. **2017**, *7*, 7644. (c) Gasparello, J.; Manicardi, A.; Casnati, A.; Corradini, R.; Gambari, R.; Finotti, A.; Sansone, F. Efficient cell penetration and delivery of peptide nucleic acids by an argininocalix[4]arene *Sci. Rep*. **2019,** *9*, 3036−3045. (d)

Ellipilli, S.; Murthy, R. V.; Ganesh, K. N. Perfluoroalkylchain conjugation as a new tactic for enhancing cell permeability of peptide nucleic acids (PNAs) via reducing the nanoparticle size, *Chem. Commun*. **2016**, 521−524. (e) Bhingardeve, P.; Madhanagopal, B. R.; Naick, H.; Jain, P.; Manoharan, M.; Ganesh, K. N. Receptor-specific delivery of peptide nucleic acids conjugated to three sequentially linked N-acetyl galactosamine moieties into hepatocytes, *J. Org. Chem*. **2020**, *85*, 8812-8824.

10. (a) Mitra R.; Ganesh, K. N. PNAs grafted with (α/γ, *R*/*S*)-aminomethylene pendants: Regio and stereospecific effects on DNA binding and improved cell uptake, *Chem Commun*. **2011**, *47*, 1198−1200. (b) Mitra, R.; Ganesh, K. N. Aminomethylene Peptide nucleic acid (am-PNA): synthesis, regio-/ stereospecific DNA binding, and differential cell uptake of (α/γ, *R*/*S*) *am*-PNA analogues, *J. Org. Chem*. **2012**, *77*, 5696−5704. (c) Jain, D. R.; Ganesh. K. N. Clickable Cγ-azido(methylene/butylene) peptide nucleic acids and their clicked fluorescent derivatives: synthesis, DNA hybridization properties, and cell penetration Studies *J. Org. Chem*. **2014**, *79*, 6708−9577. (d) Ellipilli, S.; Palvai, S.; Ganesh, K. N. Fluorinated peptide nucleic acids with fluoroacetyl side chain bearing 5-(F/CF_3)-uracil: Synthesis and cell uptake studies, *J. Org. Chem*. **2016**, *81*, 6364−6714.

11 (a) Dragulescu-Andrasi, A.; Rapireddy, S.; Frezza, B. M.; Gayathri, C.; Roberto R. Gil, R. R.; Ly, D. H. A Simple gamma-backbone modification preorganizes peptide nucleic acid into a helical structure, *J. Am. Chem. Soc*. **2006,** *128*, 10258–10267. (b) Ishizuka, T.; Yoshida, J.; Yamamoto, Y.; Sumaoka, J.; Tedeschi, T.; Corradini, R.; Stefano Sforza, S.; Komiyama, M. Chiral introduction of positive charges to PNA for double-duplex invasion to versatile sequences, *Nucleic Acids Res*. **2008**, *36*, 1464–1471.

12. (a) Govindaraju, T.; Kumar, V. A.; Ganesh, K. N. (1*S*,2*R*/1*R*,2*S*)-*cis*-cyclopentyl PNAs (*cp*PNAs) as constrained PNA analogues: synthesis and evaluation of *aeg*-*cp*PNA chimera and stereopreferences in hybridization with DNA/RNA, *J. Org. Chem.* **2004**, *69*, 5725-5734 (b) Cyclohexanyl Peptide Nucleic Acids (chPNAs) for preferential RNA binding: effective tuning of dihedral angle in PNAs for DNA/RNA discrimination, T. Govindaraju, V. Madhuri, V. A. Kumar and K. N. Ganesh, *J. Org. Chem*, **2006**, *71*, 14-21. (c) Synthesis of Fmoc-Protected (*S*,*S*)-*trans*-Cyclopentane Diamine Monomers Enables the Preparation and Study of Conformationally Restricted Peptide Nucleic Acids, Zheng, H.; Saha, M.; Appella, D. H. *Org. Lett*. **2018**, *20*, 7637–7640. (d) Hydrophilic and Cell-Penetrable Pyrrolidinyl Peptide Nucleic Acid via Post-synthetic Modification with Hydrophilic Side Chains, Suparpprom, C.; Nuanyai,

T.; Pansuwan, H.; Vilaivan, T.; Wanichwecharungruang, S.; Ditmangklo,B.; Palaga, T.; Pan-In, P.; Jiangchareon, B.; Chotima Vilaivan, C. *Bioconj. Chem*. **2017**, *28*, 2284-2202.

13 Gupta, M. K**.** Madhanagopal, B. R. Datta, B.; Ganesh, K. N**.** Structural Design and Synthesis of Bimodal PNA That Simultaneously Binds Two Complementary DNAs To Form Fused Double Duplexes, *Org. Lett*. **2020,** *22*, 5255-5260

14. (a) Kumar, P.; Sorinas, A. F.; Nielsen,L. J.; Slot, M.; Skytte, K.; Nielsen, A.; Jensen, M. D.; Sharma, P. K.; Vester, B.; Petersen, M.; Nielsen, P. Double-coding nucleic acids: Introduction of a nucleobase sequence in the major groove of the DNA duplex using double-headed nucleotides, *J. Org. Chem* **2014**, *79*, 8020 (b) Mick; H.; Julie, S.; Sharma, P K.; Pawan, K; Nielsen, P.; Rasmus B. Michael, P.; Nielsen, P. Base-pairing properties of double-headed nucleotides *Chemistry, A European Journal* **2019**, *25*, 7387-7395.

15 (a) Branda, N.; Lehn, J.-M. Janus wedges: A new approach towards nucleobase-pair recognition. *Chem. Commun*. **1996**, 2443–2444. (b) Hang, Z.; Wen, H.; Xiaohua, W.; Yong, Q.; Zhihua, X.; Yang, H. Synthesis of a complete Janus-type guanosine-cytosine base and its 2'-deoxyribonucleoside, *Chem. Lett*. **2011,** *40*, 684–686. (c) Chen, H.; McLaughlin, M.; McLaughlin, L. M. A Janus-wedge DNA triplex with A-W1-T and G-W2-C base triplets, *J. Am. Chem. Soc*. **2008**, *130*, 13190–13191. (d) Shin, D.; Tor, Y. Bifacial nucleoside as a surrogate for both T and A in duplex DNA, *J. Am. Chem. Soc*. **2011**, *133*, 6926–6929. (e) Artigas, G.; Marchan, V. Synthesis of Janus compounds for the recognition of G-U mismatched nucleobase pairs, *J. Org. Chem*. **2013**, *78*, 10666–10677.

16. (a) Xia, X.; Piao, X.; Bong, D. Bifacial peptide nucleic acid as an allosteric switch for aptamer and ribozyme function, *J. Am. Chem. Soc*. **2014**, *136*, 7265−7268. (b) Thadke, S. A.; Hridya, V. M.; Dinithi, J.; Perera, R.; Gil, R. R.; Mukherjee, A.; Ly, D. H. Shape selective bifacial recognition of double helical DNA. *Comm. Chem*. **2018,** *1*, 79. (c) Thadke, S. A. et al. Design of bivalent nucleic acid ligands for recognition of RNA-repeated expansion associated with Huntington's disease, *Biochemistry* **2018**, *57*, 2094–2108.

17. Jain, D. R.; Ganesh, K. N. Influence of pendant chiral Cγ-(alkylideneamino/guanidino) cationic side-chains of PNA backbone on hybridization with complementary DNA/RNA and cell permeability, *J. Org. Chem*. **2014**, *79*, 9567−9577.

18. (a) Bentin, T.; Hansen, G. I.; Nielsen, P. E. In Methods in Molecular Biology; Nielsen, P. E., Ed.; Humana Press Inc.: Totowa, NJ, **2002**; Vol. 208, pp 91−109. (b) Nielsen, P. E., Ed.

Peptide Nucleic Acids Protocols and Applications, 2nd ed.; Horizon Bioscience: Norfolk, UK, **2004**.

19. (a) Plum, D. E.; Park, Y-W.; Singleton, S. F.; Dervan, P. B.; Breslauer, K. J. Thermodynamic characterization of the stability and the melting behavior of a DNA triplex: A spectroscopic and calorimetric study. *Proc. Natl. Acad. Sci. U. S. A.* **1990**, *87*, 9436-9440. (b) Mergny, J. -L.; Lacroix, L. Analysis of Thermal Melting Curves, *Oligonucleotides*, **2003,** *13***,** 515–537

20. (a) Krupnik, O. V.; Guscho, Y. A.; Sluchanko, K. A.; Nielsen, P. E.; Lazurkin, Y. S. Thermodynamics of the melting of PNA_2/DNA triple helices. *J. Biomol. Struct. Dynamics* **2001**, *19*, 535-542. (b) Ratilainen, T.; Holmen A.; Tuite, E.; Nielsen, P. E.; Norden, B. Thermodynamics of sequence-specific binding of PNA to DNA, *Biochemistry* **2000**, *39*, 7781-7791 (c) Jasiński, M.; Miszkiewicz, J.; Feig, M.; Trylska, J. Thermal stability of peptide nucleic acid complexes, *J. Phys. Chem*. *B* **2019**, *123*, 8168−8177.

21. Corradini, R.; Tedeschi, T.; Sforza, S.; Marchelli, R. Electronic Circular Dichroism of Peptide Nucleic Acids and Their Analogues. In Comprehensive Chiroptical Spectroscopy, Volume 2: Applications in Stereochemical Analysis of Synthetic Compounds, Natural Products, and Biomolecules. Berova, N.; Polavarapu, P. L.; Nakanishi, K.; Woody, R. W. Eds.; John Wiley & Sons, Inc, **2012**; Vol. 2, pp 581−617.

22. (a) Xu, D.; Evans, K. O.; Nordlund, T. M. Melting and premelting transitions of an oligomer measured by DNA base fluorescence and absorption, *Biochemistry* 1994, *33*, 9592-9599 (b) Chen, Y. Z.; Prohofsky, E. W. Differences in melting behaviour between homopolymers and copolymers of DNA: Role of nonbonded forces for GC and the role of the hydration spine and pre-melting transition for AT, *Biopolymers,* 1993, *33*, 797-812. (c) Movileanu, L.; Benevides, J. M.; Thomas, Jr. G. J. Determination of base and backbone contributions to the thermodynamics of premelting and melting transitions in *B* DNA. *Nucleic Acids Res*. **2002**, *30*, 3767–3777. (d) Sobell, H. M. Premeltons in DNA. *J. Struct. Funct. Genomics,* **2016**, *17*, 17–31

23. (a) Sacui,I.; Hsieh, W.-C.; Manna, A.; Bichismita Sahu, B.; Ly, D. H. Gamma Peptide Nucleic Acids: As Orthogonal Nucleic Acid Recognition Codes for Organizing Molecular Self-Assembly, *J. Am. Chem. Soc.* **2015,** *137*, 8603–8610 (b) Manicardi, A.; Roberto Corradini, R. Effect of chirality in gamma-PNA: PNA interaction, another piece in the picture, Artificial DNA;PNA&XNA, **2014**, *5*, e1131801

24. (a) Manicardi, A.; Rozzi, A.; Korom, S.; Corradini, R. Building on the peptide nucleic acid (PNA) scaffold: a biomolecular engineering approach, *Supramol. Chem.* **2017**, *29*, 784−795. (b) Duan, T.; He, L; Tokura, Y.; Liu, X.; Wu, Y.; Shi, Z. Construction of tunable peptide nucleic acid junctions. *Chem. Commun*. **2018**, *54*, 2846−2850. (c) Swenson, C. S.; Velusamy, A.; Argueta-Gonzalez, H. S.; Heemstra, J. Bilingual peptide nucleic Acids: Encoding the languages of nucleic acids and proteins in a single self-assembling biopolymer, *J. Am. Chem. Soc*. **2019**, *141*, 19038−19047. (d) Canady, T. D.; Berlyoung, A. S.; Joe A. Martinez, J. A.; Emanuelson, C.; Telmer, C. A.; Bruchez, M. P.; Armitage, B. A. Enhanced hybridization selectivity using structured gamma PNA probes, *Molecules* **2020**, *25*, 970−982.

25. Cadoni, E.; Manicardi, A.; Madder, A. PNA-based microRNA detection methodologies, *Molecules* **2020**, *25*, 1296−1321.

26. (a) Hong, F.; Zhang, F; Liu, Y.; Yan, H. DNA Origami: Scaffolds for creating higher order structures, *Chem. Rev*. **2017**, *117*, 12584−12640. (b) Bila, H.; Kurisinkal, E. E.; Bastings, M. M. C. Engineering a stable future for DNA-origami as a biomaterial, *Biomater. Sci*. **2019**, *7*, 532−541.

27. Koch, T. PNA synthesis by Boc chemistry In Peptide Nucleic Acids: Protocols and Applications, 2nd ed.; Nielsen, P. E., Ed.; Horizon Scientific: Norfolk, UK, 2004; pp 37e59.

28. F. Debaene, J. A. DaSilva, Z. Pianowski, F. J. Duran, N. Winssinger, *Tetrahedron*, **2007**, *63*, 6577-6586.

Table of Contents Graphic